AD NUMBER

AD854941

LIMITATION CHANGES

TO:

Approved for public release; distribution is unlimited.

FROM:

Distribution authorized to U.S. Gov't. agencies and their contractors; Critical Technology; JUL 1969. Other requests shall be referred to Air Force Aero Propulsion Laboratory, Attn: APIP-2, Wright-Patterson AFB, OH 45433. This document contains export-controlled technical data.

AUTHORITY

AFAPL per DTIC form 55

LARGE RETRACTABLE SOLAR CELL ARRAY

FOURTH QUARTERLY REPORT

JULY 1969

PREPARED FOR----------

Air Force Aero Propulsion Laboratory
Research and Technology Division
Wright-Patterson Air Force Base, Ohio 45433
attn: APIP-2

PROJECT NO. 682J/DATA NO. HS207-205(4)/CONTRACT NO. F33615-68-C-1676

●

PREPARED BY:
Hughes Aircraft Company / Space Systems Division
(Under Contract F33615-68-C-1676)

AUTHORS: E. O. Felkel
G. Wolff
Et al.

Hughes Ref No. 69(22)-4490/B532-006

SSD 90240R

BLANK PAGES
IN THIS
DOCUMENT
WERE NOT
FILMED

LARGE RETRACTABLE SOLAR CELL ARRAY

FOURTH QUARTERLY REPORT

JULY 1969

PREPARED FOR
Air Force Aero Propulsion Laboratory
Research and Technology Division
Wright-Patterson Air Force Base, Ohio 45433

PROJECT NO. 682J/DATA NO. HS207-205(4)/CONTRACT NO. F33615-68-C-1676

●

PREPARED BY:
Hughes Aircraft Company / Space Systems Division
(Under Contract F33615-68-C-1676)

AUTHORS: E. O. Felkel
G. Wolff
Et al.

Hughes Ref No. 69(22)-4490/B532-006

SSD 90240R

FOREWORD

This report was prepared by Hughes Aircraft Company, Space Systems Division, El Segundo, California, under Contract F33615-68-C-1676. The work was administered under the direction of L. D. Massie, APIP-2 Air Force Aero Propulsion Laboratory.

The period covered extends from 24 March to 29 June 1969. Contributors to this report include E. O. Felkel, G. Wolff, M. C. Olson, W. N. Turner, R. E. Daniel, G. P. Steffen. G. Serbu, D. Plummer, D. Creed, C. Duncan, and D. Lane, all of Hughes Aircraft Company, Space Systems Division, El Segundo, California.

The work covered herein was accomplished under Air Force Contract F33615-68-C-1676, but this report is being published and distributed prior to Air Force review. Publication of this quarterly, therefore, does not constitute approval by the Air Force of the findings or conclusions contained herein. It is published for the exchange and stimulation of ideas.

ABSTRACT

The main activity on the Large Retractable Solar Cell Array (LRSCA) program during the fourth quarterly reporting period consisted of completion of the detail drawings of the orientation mechanism, start of incorporating reference solar cell and solar cell modules consisting of 8- and 12-mil cells in the solar panel design, and near completion of the detail drawings of the drum mechanism and solar array. All electronic circuit detail design has been completed. Breadboards of the solar panel switch and charge current controller have been built and successfully tested over the anticipated orbital temperature extremes. The breadboard and engineering models of the boom actuator and their respective test programs have been completed by Spar Aerospace Corporation.

A power management summary has been prepared, and the preliminary "Performance, Design, and Product Confirmation Requirements for HS-207 Large Retractable Solar Cell Array Experiment" and the preliminary "Interface Requirements for HS-207 Large Retractable Solar Cell Array Experiment" have been revised to reflect the present LRSCA design.

A major accomplishment has been the resolution of uncertainties regarding the array dynamics and control/structural interactions. A review of the system dynamic characteristics and Hughes' analytic treatment of this field was presented to the Working Group on Flexible Vehicle Dynamic Interactions of the Joint USA/United Kingdom Technical Coordination Program (M-4) as the LRSCA program second semiannual presentation.

Coordination with Lockheed Missiles and Space Company (LMSC), designated as the mission study integration contractor, was initiated on 17 June 1969.

CONTENTS

ILLUSTRATIONS

TABLES

SECTION I

INTRODUCTION AND SUMMARY

This document reports the progress in the fourth quarter (24 March to 29 June 1969) on AFAPL Contract F33615-68-C1676, Large Retractable Solar Cell Array, Project 682J.

The main activity on the Large Retractable Solar Cell Array (LRSCA) program during the fourth quarterly reporting period consisted of completion of the detail drawings of the orientation mechanism, start of incorporating reference solar cell and solar cell modules consisting of 8- and 12-mil cells in the solar panel design, and near completion of the detail drawings of the drum mechanism and solar array. All electronic circuit detail design has been completed. Breadboards of the solar panel switch and charge current controller have been built and successfully tested over the anticipated orbital temperature extremes. The breadboard and engineering models of the boom actuator and their respective test programs have been completed by Spar Aerospace Corporation.

A power management summary has been prepared, and the preliminary "Performance, Design, and Product Confirmation Requirements for HS-207 Large Retractable Solar Cell Array Experiment" and the preliminary "Interface Requirements for HS-207 Large Retractable Solar Cell Array Experiment" have been revised to reflect the present LRSCA design.

A major accomplishment has been the resolution of uncertainties regarding the array dynamics and control/structural interactions. A review of the system dynamic characteristics and Hughes' analytic treatment of this field was presented to the Working Group on Flexible Vehicle Dynamic Interactions of the Joint USA/United Kingdom Technical Coordination Program (M-4) as the LRSCA program second semiannual presentation.

Coordination with LMSC, designated as the mission study integration contractor, was initiated on 17 June 1969.

The format of this report is designed to present the status of each major system element in a separate section.

SECTION II

PROGRAM STATUS

The Large Retractable Solar Cell Array (LRSCA) program is divided into five phases, as described in the paragraphs that follow. The current program schedule and status are shown in Figure 1.

PHASE I – PROGRAM DEFINITION

Major milestones associated with this phase and scheduled during this period have been completed. Included in this category are preliminary releases of the life test requirements plan, system design specification, engineering model test plan and procedures, and instrument subsystem design specification. The final interface specification, qualification model design and test specification, and the orbital experiment plan will be completed early in the next quarter.

PHASE II – DESIGN STUDY AND ANALYSIS

The program has been modified to incorporate reference solar cells and solar cell modules including both 8- and 12-mil cells, and the addition of instrumentation to the second panel similar to that which had been incorporated in panel 1.

All tradeoff studies have been completed, preliminary design reviews held, and a firm baseline established. Presently, all elements of the system are in the detail design and development hardware fabrication phases. Development test models of the orientation mechanism and the flexible array subsystem, as well as all electronic breadboards, will be completed during the next quarter.

A major accomplishment in the program has been the analysis of the dynamic interaction between the large flexible appendage and the orientation mechanism control system which proves that the system will remain stable.

The principal problem experienced by the program has been delay by the Air Force in choosing a vehicle integration contractor, making it impossible for Hughes to finalize interface design requirements. This problem, however, is being resolved. The Air Force (SESP Office) has awarded a mission integration study contract to LMSC, Sunnyvale. The first WPAFB/SAMSO (SESP Office)/LMSC/Hughes interface meeting was held at the Hughes facilities on 17 June 1969.

PHASE III – MODEL FABRICATION

Spar Aerospace Products, Ltd., Canada, has completed the fabrication of the engineering model and the breadboard model of the boom actuator units. Both the breadboard test and the engineering model test programs have been completed. The acceptance test program is now in progress, and the engineering model will be delivered to Hughes in the next quarter.

PHASE IV – QUALIFICATION AND FLIGHT ACCEPTANCE TESTS

Qualification and flight acceptance tests will be conducted according to the General System Test Plan, which includes formalized qualification tests, acceptance tests, and environmental tests.

PHASE V – FLIGHT TEST AND DATA ANALYSIS

The flight test and data analysis phase will include prelaunch checkout and countdown procedures, as well as in-orbit operation and analysis.

Data analysis format and requirements have been forwarded to LMSC as a requirement of the integration task.

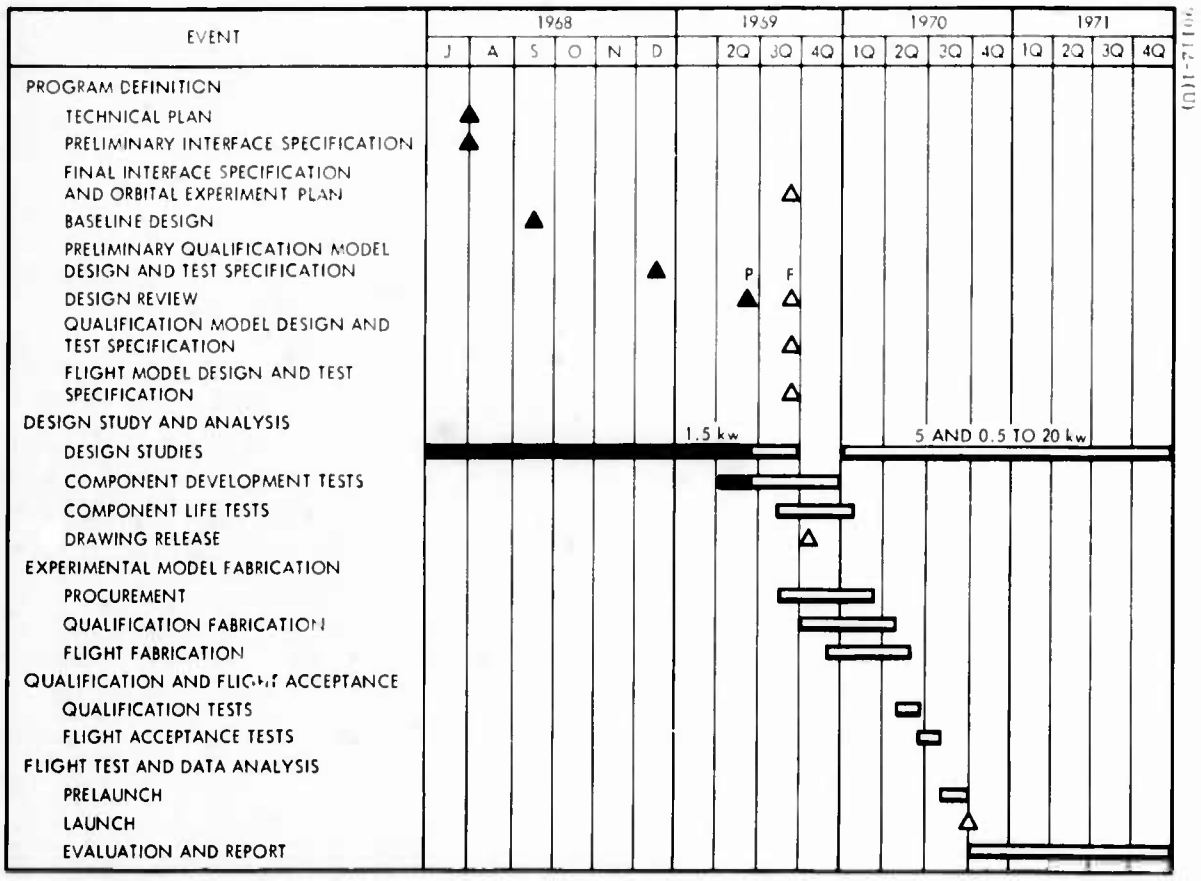

Figure 1. Program Schedule

SECTION III

SYSTEMS ENGINEERING

DESIGN AND INTERFACE REQUIREMENTS SPECIFICATIONS

The preliminary DS 30992-001 Specification, "Performance, Design and Product Confirmation Requirements for HS-207 Large Retractable Solar Cell Array Experiment" has been updated to reflect recent design changes. The specification defines general functional, design and test requirements for each control item, system and the complete LRSCA system. This document will be updated as the design evolves and as the launch vehicle and mission parameters become more firmly established. Since launch vehicle interface meetings did not commence until 17 June 1969, the target release date for this document has been moved back to 1 September 1969.

The preliminary ICD 30992-002 Specification, "Interface Requirements for HS-207 Large Retractable Solar Cell Array Experiment" has been revised to reflect the present LRSCA design and submitted to Lockheed for review during the initial interface meeting. This document describes all mechanical, electrical, and thermal interfaces between the LRSCA experiment and the Agena vehicle. Target release date for the final interface specification is 1 September 1969.

POWER MANAGEMENT SUMMARY

A preliminary power management summary which lists the power dissipation for all configurations that will be encountered in orbit has been prepared. This document is needed in order to perform mission planning, conduct thermal analyses, evaluate battery performance, etc. The power management summary indicates dissipation by subsystem for the following mission configurations

1) Launch (battery-powered)

2) Initial array extension with control electronics turned off (battery-powered)

3) Sun tracking (normal illumination with solar panels supplying power)

4) Array panel retraction and extension (battery-powered)

5) Eclipse operation (battery-powered)

Eclipse system power requirements are approximately 1 A-H. Maximum sunlight requirements are approximately 180 watts.

COMMAND LIST

The addition of the solar cell electronics unit to the instrumentation subsystem has resulted in the addition of one command. Table I lists all current commands required by LRSCA from the Agena command decoder.

LRSCA WEIGHT SUMMARY

A current system weight summary is shown in Table II. Changes in system weight were due to the following:

1) Increase of 1.6 pounds in the orientation linkage subsystem due to the selection of large diameter, more efficient motors

2) Decrease of 3.2 pounds in the solar array subsystem due to the use of thinner cells

3) Increase of 15.2 pounds in the power conditioning and storage subsystem as a result of system reconfiguration

4) Increase of 1.93 pounds in the instrumentation subsystem due to the increase in the number of strain gauges and accelerometers

The weights shown under categories II, III, and IV have not been shown in previous quarterly reports since it was felt that they do not represent basic system weight.

TABLE I. LRSCA COMMAND LIST

Command	Command Function
1	Manual torque support X-axis, OFF/Plus Positive
2	Manual torque support X-axis, OFF/Minus Negative
3	Manual torque drum W-axis, OFF/Plus Positive
4	Manual torque drum W-axis, OFF/Minus Negative
5	Control electronics unit, OFF/ON
6	Limit override, OFF/ON
7	Solar array power switch, Disable
8	Solar array power switch, Enable

Table I (continued)

Command	Command Function
9	Overvoltage-undervoltage override, OFF
10	Overvoltage-undervoltage override, ON
11	Solar array, Extend
12	Solar array, Retract
13	Solar array motor, Disable
14	Solar array motor, Enable
15	Battery charge, Disable, OFF
16	Battery charge, Enable, ON
17	Load bank 1, ON
18	Load bank 2, ON
19	Load bank 3, ON
20	Load bank 4, ON
21	Load bank 1, OFF
22	Load bank 2, OFF
23	Load bank 3, OFF
24	Load bank 4, OFF
25	Sun lockon override, Enable
26	Sun lockon override, Disable
27	Release and extend logic override, Enable
28	Release and extend logic override, Disable
29	Retract logic override, Enable
30	Retract logic override Disable
31	Manual sun lockon, OFF/ON
32	Manual sun present, OFF/ON
33	Torquer drive, AUTO/OFF
34	Solar cell experiment, OFF/ON

TABLE II. LRSCA FLIGHT WEIGHT SUMMARY

Category	Subsystem	Weight, pounds		
	Orientation Linkage			
	Structure		17.6	
	Controls and avionics		19.9	
	Motors and tachometers	12.0		
	Sun sensors	0.7		
	Electronics	7.2		
	Power and signal transfer		8.3	
	Sliprings/brushes	6.6		
	Wire and connectors	1.7		
	Subsystem total			45.80
	Solar Array			
	Solar array panel		34.76	
	Cells with covers	28.90		
	Cells Z-strips	1.60		
	Fiberglass and adhesive	1.34		
	Kapton substrate	1.41		
	Power bus	1.51		
	Array cushion, reel, and drive		2.12	
	Drum mechanisms		33.40	
	Drum, spar, and thermal covers	11.38		
	Actuators	16.52		
	Power harnesses and hardware	2.85		
	Boom length compensators	0.60		
	Spreader bar	2.05		
	Subsystem total			70.28

Table II (continued)

Category	Subsystem	Weight, pounds	
	Power Conditioning and Storage		
	Batteries	43.0	
	Control electronics	17.0	
	Subsystem total		60.00
	Instrumentation		9.38
I	LRSCA System Total		185.46
II	Solar Cell Reference Modules		
	Commutator, electronics, connectors		2.94
III	Installation Equipment		38.92
	Load bank	35.00	
	Orbital rack fittings	3.92	
IV	Contingency		22.68
	Total flight weight		250.00

SECTION IV

SOLAR ARRAY SUBSYSTEM

SUBSYSTEM DESCRIPTION AND STATUS

The solar array subsystem consists of two flexible solar cell arrays that are stored, deployed, and retracted by the storage drum mechanisms (Figure 2).

During the fourth quarter of the program, the following significant items and tasks were accomplished:

1) Completion of 95 percent of detail drawings for drum mechanisms and solar arrays

2) Completion of boom actuator unit engineering model development test program

3) Completion of drum drive negator test equipment modifications for high and low-temperature life tests

4) Completion of fabrication, electrical testing, and rollup evaluation of vibration test panels and cushion

5) Start of development program to emboss full-size kapton cushions

6) Completion of room temperature life tests on contoured drum negators

7) Completion of solar array materials and processes test program

8) Completion of fabrication on thermal shock and cycling test samples of solar array

STORAGE DRUM MECHANISMS

Boom Actuators

A design review was held at Spar Aerospace in Toronto, Canada, on 9 April 1969. The purpose of the review was to evaluate the design of the

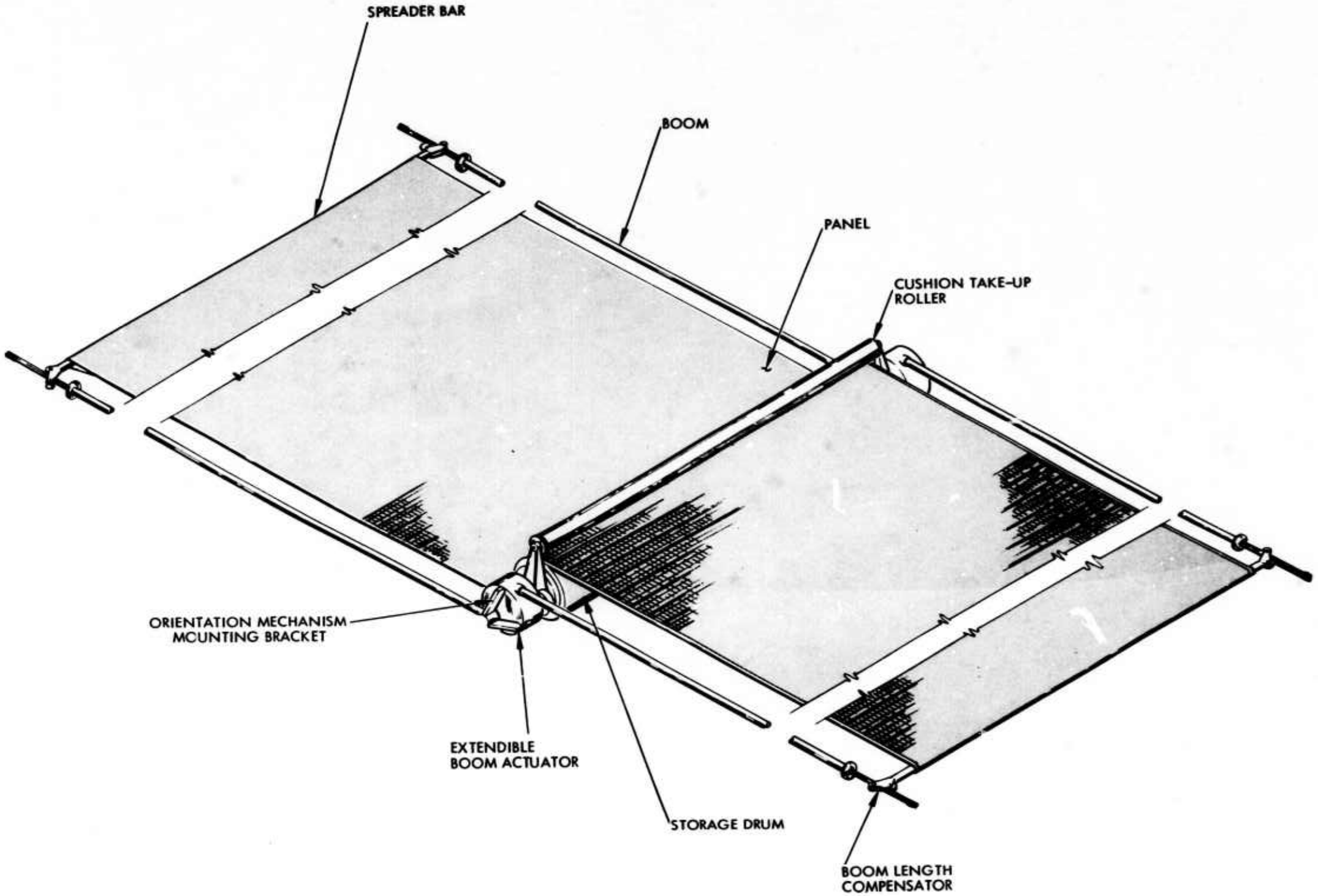

Figure 2. Solar Array Subsystem

boom actuator unit and provide answers to several questions generated at the Hughes solar array subsystem design review held last month. The principal topics discussed concerned the following:

1) Verification of boom thermal deflection

2) Gear and bearing lubrication plans for engineering model as well as flight units

3) Cleaning and maintaining silver plating on booms during test, etc.

4) Wear and debris generation in actuator during extension/retraction

5) Adequacy of motor torque margins

6) Effect of microswitch failure on actuator and bi-STEM element

7) Humidity protection of dry-lubricated parts during assembly and test shipping

The breadboard model of the boom actuator unit has been built and subjected to a life test program. This program consisted of 314 extensions and retractions with simulated tip loading. The successful demonstration of 314 cycles represents a capability to perform 35 cycles with a 90 percent confidence level.

A completely representative unit called the engineering model has also been fabricated and subjected to a development test program. The program consisted of a thermal test, vibration test, and a series of functional tests concerned with boom synchronization, straightness, deflection, etc. The unit is scheduled for delivery to Hughes early next month for use in the solar array subsystem engineering model test effort.

Storage Drum Negators

The test equipment for the bearing and negator development test program has been reworked to add automatic cycling provisions. This feature was considered necessary to adequately evaluate the negator torque characteristics as a function of number of cycles. Additional changes were also made to facilitate electrical monitoring of torque over the entire travel range.

A contoured negator was subjected to more than 4450 cycles in the modified test setup at room temperature before failure occurred. This represents a large margin over the 2500-cycle vendor guarantee and the 35-cycle (10 flight plus 25 preflight ground test) life required for the experiment. Measurements made after about 4000 cycles revealed no apparent change in the negator torque characteristics over a typical cycle. These measurements also indicated that the contouring operation is achieving the features desired.

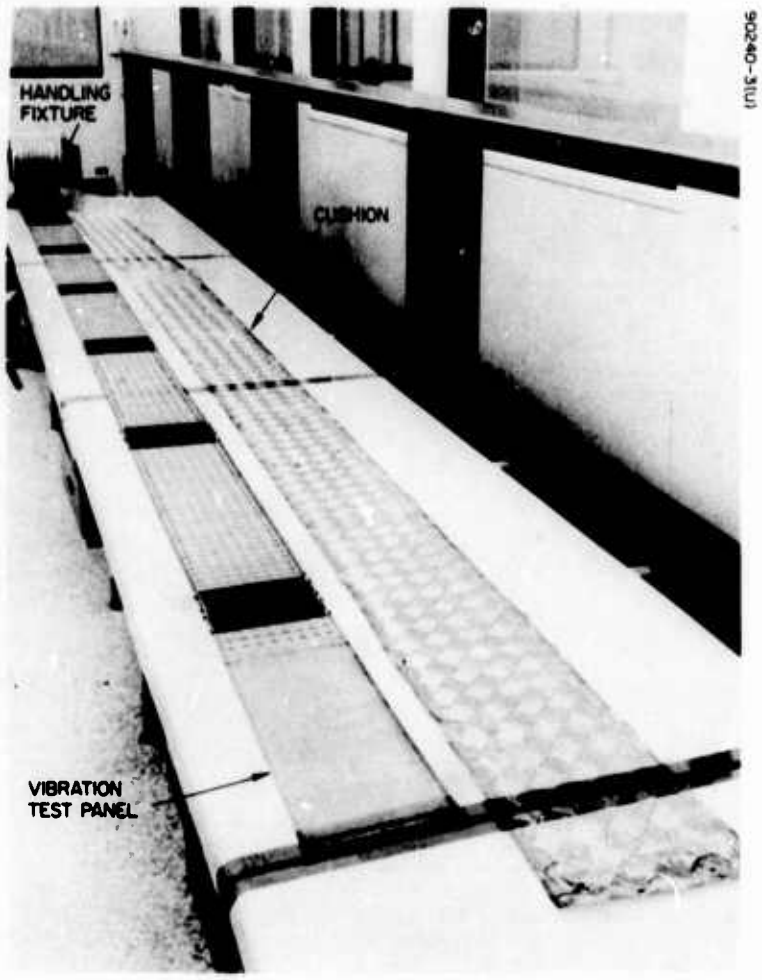

Figure 3. Vibration Test Solar Array and Cushion

(Photo A24335)

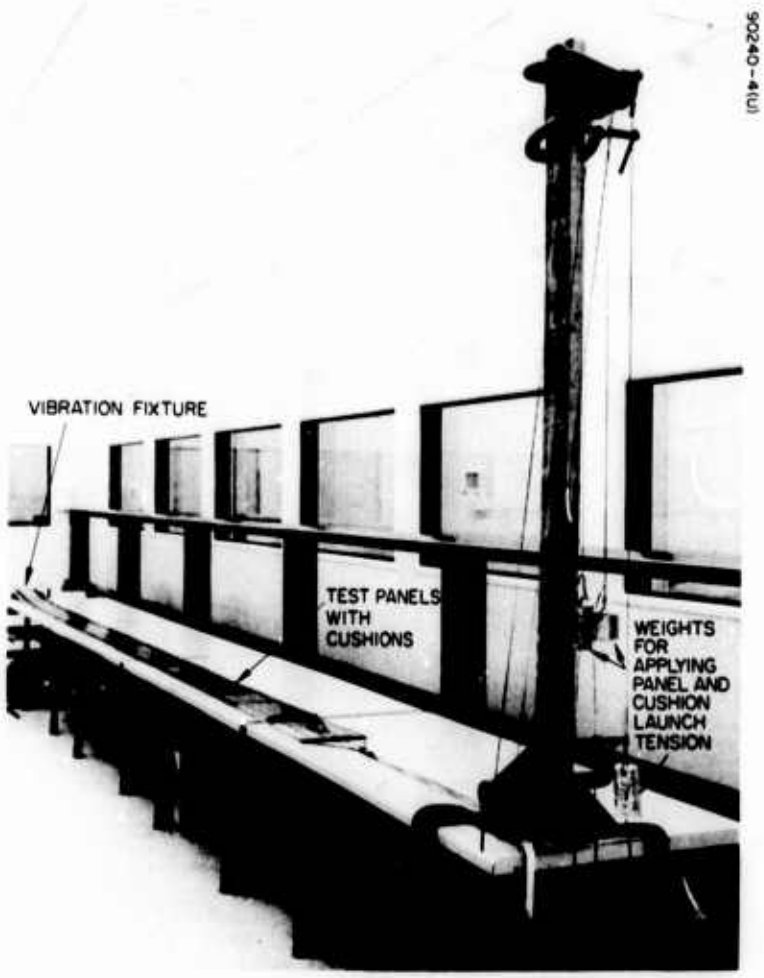

Figure 4. Setup for Applying Launch Tension During Panel Rollup

(Photo A24337)

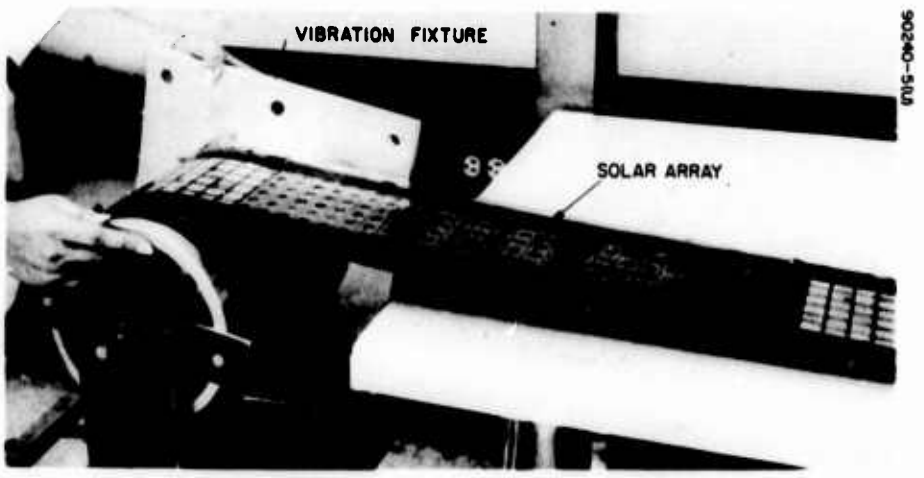

Figure 5. Solar Panels and Cushion Being Rolled up on Vibration Fixture

(Photo A24338)

Following the room temperature life test, the setup was dismantled for incorporation of 1) provisions for supplying and recirculating heated dry nitrogen within test enclosure, and 2) equipment for cooling the enclosure with liquid nitrogen that is required for low-temperature tests.

Design Task

The detail drawings of the drum mechanism are about 95 percent complete. Stress analysis and check have been completed on about 75 percent of the completed drum mechanism drawings. The following are the most significant design changes incorporated since the last reporting period:

1) Storage drum fabrication procedure changed from a chemical milled extruded tube to a welded sheet construction. This change reduces fabrication costs and time without appreciably affecting the structural characteristics of the part.

2) Incorporation of lightening holes in storage drum to reduce weight. The stress analysis performed on the drum provided the data necessary to facilitate this change.

3) Modification of output reel for the drum negator drive. This change resulted from interference problems observed during the negator development test program.

The primary objective of the design task at the present time is to complete the check and stress analysis of the long-leadtime parts required for the engineering model. These parts include such items as the drum, drum end bulkheads, drum spar, and cushion reel supports.

FLEXIBLE SOLAR ARRAY

Panel Vibration Tests

The panels and cushion for vibration testing of the flexible array have been completed (Figures 3, 4, and 5). A complete mechanical and electrical inspection has been performed on the live-cell portion of the specimens. The panels and cushion have been rolled up several times on an 8-inch-diameter vibration fixture with launch tension applied. The purpose of this effort was to determine the number of turns required to roll up 16-foot-long panels, the envelope diameter of the stowed panels, the difference between panel lengths due to interleaving of cushion, and the effect of repeated rollups on stowed parameters.

The test panels and cushion are presently rolled up on the vibration fixture with launch tension applied, ready for testing to the Titan IIIC random vibration environment as soon as facilities are available.

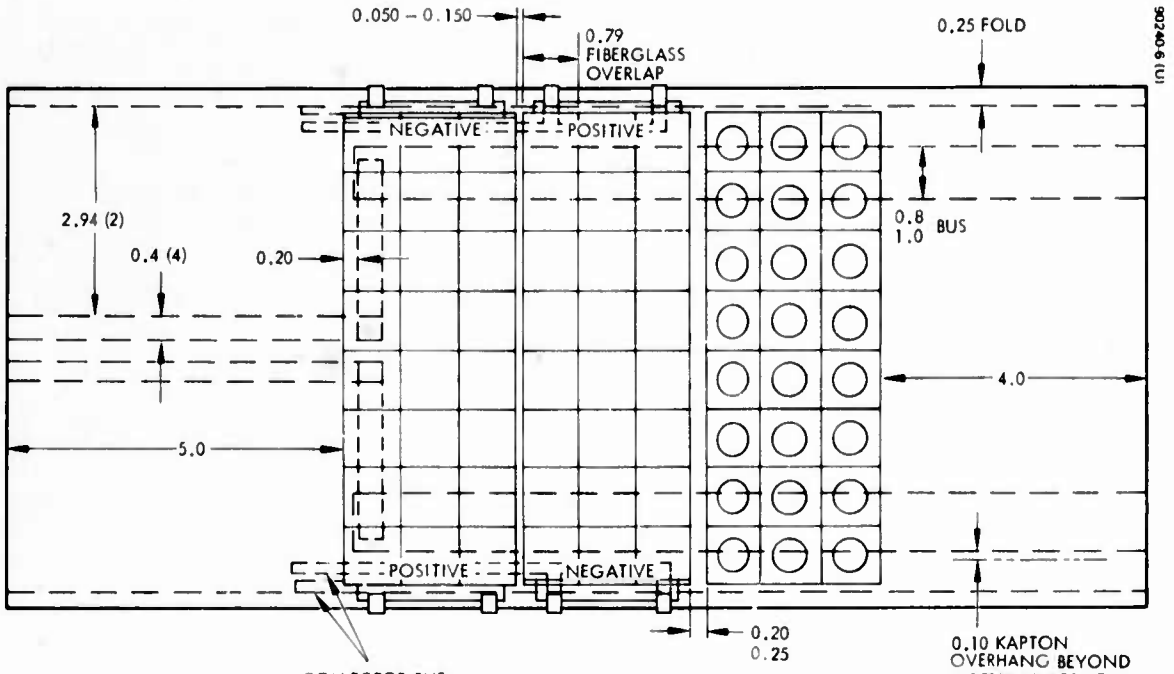

Figure 6. Layout of Solar Array Thermal Shock and Cycling Test Specimens

Thermal Shock and Cycling Tests

The thermal cycling test program, designed to subject sample segments of a panel to rapidly changing temperature environments, is currently under way. The configuration for the test specimens has been determined (see Figures 6, 7, and 8) and fabrication completed. Since one of the critical areas in the panel may be at the interface between live and dummy aluminum cells, all samples planned for this program will contain both 8-mil live cells and aluminum dummy cells. The number of cycles and temperature rates of change are currently being investigated.

PLANS FOR NEXT QUARTER

1) Completion of stress analysis

2) High and low-temperature tests of drum drive negators

3) Start of fabrication of solar array subsystem engineering model

4) Start of cycling tests on solar array segments

5) Preparation of procurement documentation for flight and qualification unit solar cells

6) Release of detail drawings for flight and qualification units

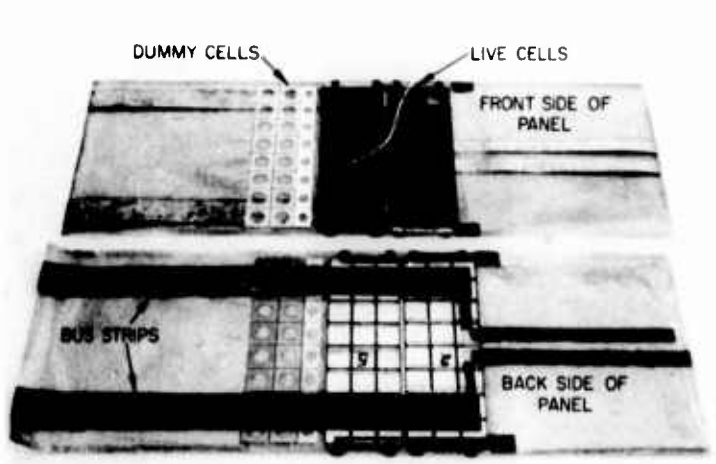

Figure 7. Solar Array Thermal Shock and Cycling Test Specimens

(Photo A24339)

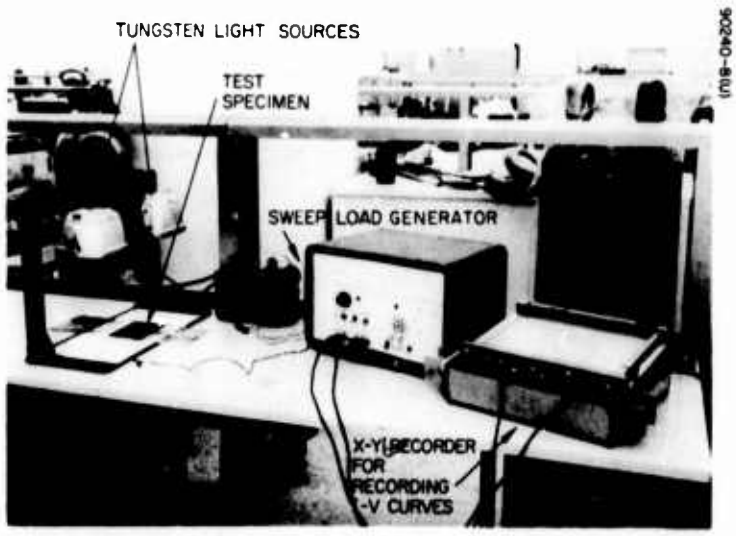

Figure 8. Electrical Test Setup for Solar Array Test Specimens

(Photo A24340)

SECTION V

ORIENTATION MECHANISM

SUMMARY

During this quarter, the detailed drawings of the orientation mechanism (OLSCA) were completed. Uncertainties regarding array dynamics and control/structural interactions were resolved.

Formal reviews of the mechanism and the control system functional designs were conducted, and resulting minor modifications incorporated as appropriate. A review of the system dynamic characteristics and Hughes' analytic treatment of this field was presented to the Working Group on Flexible Vehicle Dynamic Interactions of the Joint USA/United Kingdom Technical Coordination Program. Coordination with the mission integration contractor was initiated.

DETAIL DESIGN

Drawings defining details of the mechanism design are essentially complete. Checking and part stress analysis have been started.

A review of the orientation linkage mechanical design was held on 28 March. The resulting action items, which have been implemented in the design, were:

1) Properly venting the housing assembly to ensure that outflow during launch ascent avoids the bearings

2) Configuring the accelerating and snubbing springs in the deployment mechanism so that the decelerating spring can be eliminated

DYNAMICS AND STRESS

As part of the general review of interaction of panel dynamics with the linkage control system, updated values were computed for the panel dynamic transfer functions, i.e., the expressions defining reaction torques induced on the OLSCA axes by the flexible panels in response to control torque inputs. The model used for derivation of these expressions comprised the two booms (per panel), the spreader bar across the boom ends, and the panel itself modeled as a string (or membrane incapable of supporting shear) in tension.

Transfer functions were obtained for the following configuration.

Panel	90 ft^2, 5.62 feet wide at 0.22 lb/ft^2
Boom	0.86 inch diameter by 5 mils thick; stainless steel
Spreader	0.47 lb/ft
Panel tension	4 pounds total (2 pounds per boom)

Two panels are mounted on the drum axis with the center line of the panels located at 6.62 feet from the support axis.

The expressions summarized below contain only contributions from the panel assembly. Contributions from drum assembly, drive mechanism, and shafting (weighing approximately 35 pounds) are not included in these tabulated values.

Contributions from the panels to equations of motion about the drum axis φ and about the support axis are as follows: (with all modes normalized so that $M_{bi}(3,3)$ and $M_{ti}(3,3)$ equal unity)

$$2\left\{M_b(2,2) - \sum i \frac{[M_{bi}(2,3)]^2}{1 + (\omega_{bi}/S)^2}\right\} \ddot{\varphi} = M_\varphi$$

$$2\left\{R^2 M_b(1,1) + \sin^2\varphi \left[M_b(2,2) - \sum i \frac{[M_{bi}(2,3)]^2}{1 + (\omega_{bi}/S)^2}\right]\right.$$

$$\left. + \cos^2\varphi \left[M_t^*(1,1) - \sum i \frac{R^2 [M_{bi}(1,3)]^2}{1 + (\omega_{bi}/S)^2}\right] - \sum i \frac{(h/2)^2 [M_{ti}(1,3)]^2}{1 + (\omega_{ti}/S)^2}\right\} \ddot{\psi}$$

$$= M_\psi$$

$M(1,1)$ = panel mass

$M(2,2)$ = panel moment of inertia about the drum axis

$M(1,3)$, $M(2,3)$, $M(3,3)$ = mass coupling terms where index 1 denotes uniform lateral displacement of the rigid panel, index 2 denotes motion corresponding to a root rotation about the drum axis, and index 3 stands for motion due to a normal mode of the panel

ω = frequency of panel motion

S = Laplace transform

φ = angle about drum axis

Ψ = angle about OLSCA support axis

h = panel width

R = distance from OLSCA support axis to center of panel

i = summation over the frequencies

b, t = indices for bending and torsional mode respectively

The values for the M-terms are calculated in a digital computer program.

Values of M for i up to 3 are given in Table III. Subscript (i) refers to the order of the modules. The angle φ is measured about the drum axis from a reference position when the plane of the panels contains the support axis.

$$R = 6.62 \text{ feet}$$

$$h/2 = 5.62/2 = 2.81 \text{ feet}$$

$$M_b(1,1) = 0.7616 \text{ slug}$$

$$M_b(2,2) = 79.13 \text{ slug-ft}^2$$

$$M_t^*(1,1) = (2.81)^2 \times (0.2968) = 2.345 \text{ slug-ft}^2$$

CONTROL SYSTEM

Further analysis of peculiarities that were thought to exist in the model for motion about the support axis, reported in the third quarterly report, have been resolved by correction of errors in a computational program

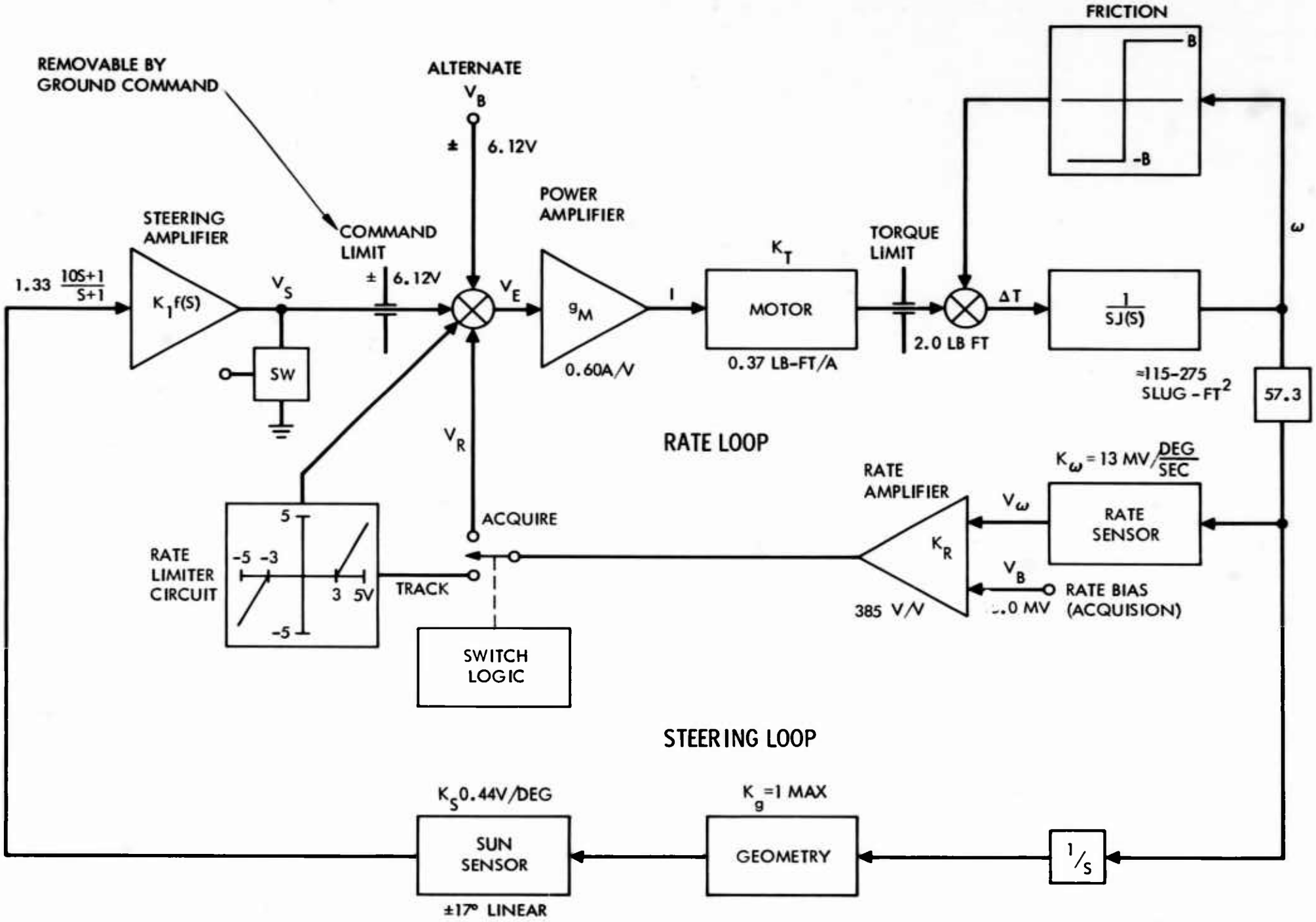

Figure 9. Functional Schematic of One Axis of Array Control System

TABLE III. VALUES OF M

i	1	2	3
$M_{bi}(1,3)$	0.7889	0.1845	0.1522
$M_{bi}(2,3)$	8.7179	-1.5602	0.0612
f_{bi}, (cps)	0.1796	0.4328	0.7063
(R/S)	1.1284	2.7193	4.4378
$M_{ti}(1,3)$	0.4826	-0.00014	0.1773
f_{ti}, (cps)	0.1911	0.4649	0.7569
(R/S)	1.2009	2.9211	4.7555

and an algebraic reduction procedure. Consistent, logical, and tractable data are now obtained and the system remains stable, as was previously concluded. As a backup, a separate analysis of the fundamental phenomena acting in a flexible dynamic system of this type was developed which clearly indicated that consistency of results and a stable order of the flexible-mode transfer function poles and zeros were to be expected. This type of dynamic system means: 1) one in which the torquers and sensors are located at effectively the same place on the structure (base of the arrays) so that flexible mode shapes do not introduce extraneous phase relationships, and 2) the control system does not contain integral compensation.

Analysis

A functional schematic of one axis of the array control system is illustrated in Figure 9. If the control circuit is linearized by omitting the OLSCA coulomb friction from the model, the open-loop Bode plot of Figure 10 describes the system. The characteristics at frequencies below 1 rad/sec are seen to be well-behaved, with over 50 degrees of phase margin in the gain crossover region. Above 1 rad/sec, the effects of the lower frequency array flexibility modes are apparent in terms of plus and minus 180-degree shifts in phase and an irregular gain curve resulting from the recurring zero/pole pairs of the transfer function. The graph is drawn for the first two such pairs; others follow ad infinitum. The general effect, when the structural zeros and poles occur in this order, is to shift the average phase angle in a favorable direction. It is necessary, however, to ensure that a positive phase margin exists in regions where the gain rises again above the zero dB level, i.e., at the system's poles. Structural damping introduces a favorable effect but, at the low values characteristic of the lower modes, this is seen to be slight.

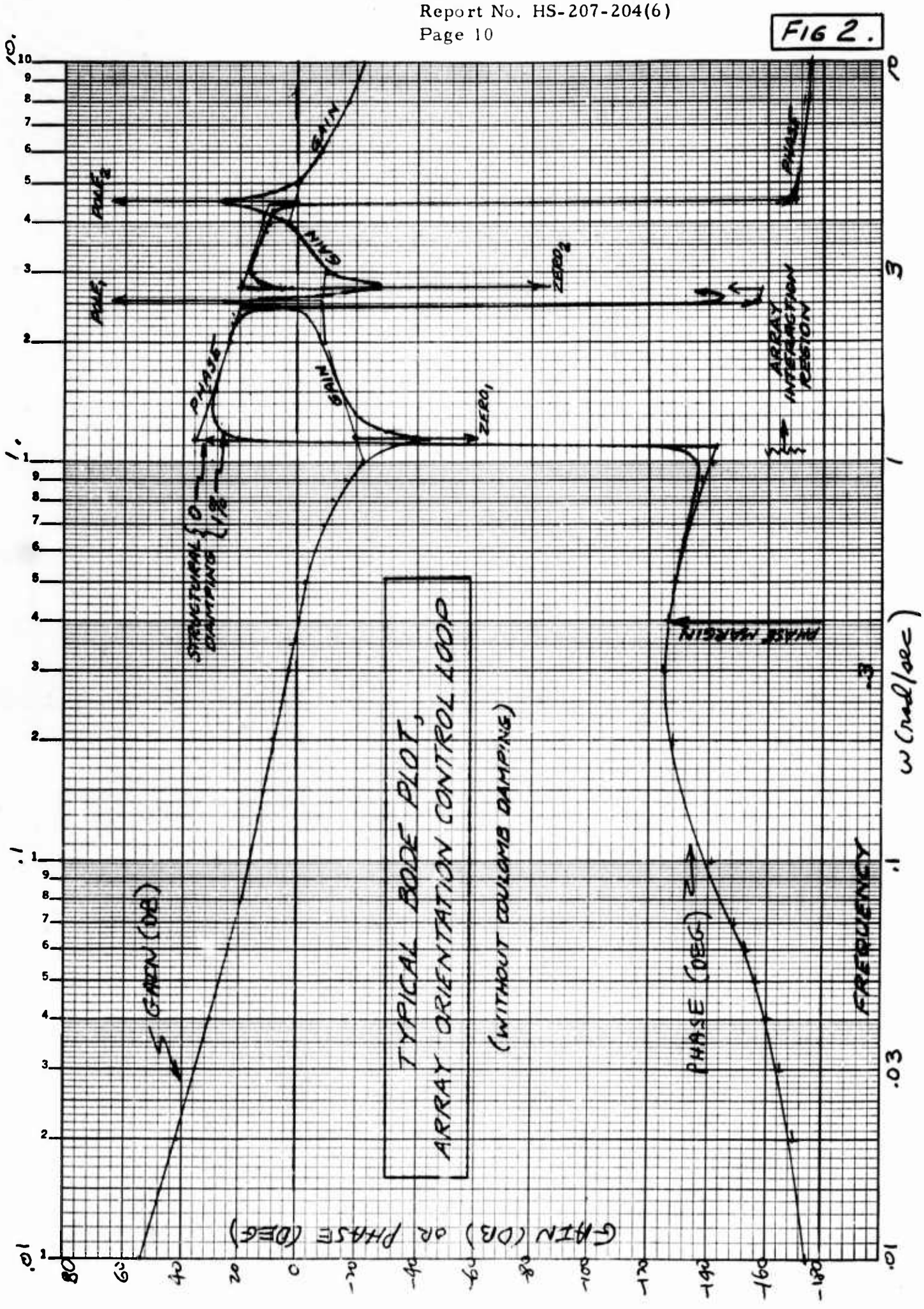

Figure 10. Typical Bode Plot, Array Orientation Control Loop

The general trend of the baseline phase curve is toward very low values of phase margin as frequency increases in this region. Two factors not included in the model tend to counter this potential problem:

1) The characteristic increase in structural damping with mode

2) The contribution of the nonlinear coulomb friction in the OLSCA assembly (brush drag and bearing friction). The coulomb friction contributes damping only at near-zero average rates because the oscillatory component must undergo reversals, but most of the systems' operation is in this region. Coulomb damping increases linearly with friction level and oscillation frequency.

Eventually, higher-order lags arising in the control electronics and torquers will introduce additional phase shift, but accompanying gain attenuation at these frequencies will maintain system stability.

Performance

The analog computer provides the most valid indication of actual system performance with coulomb friction and other nonlinearities included. Figure 11 illustrates the performance in sun acquisition, and Figure 12, in noon turns. Normal tracking performance is evident at the end of each of the maneuvers. The two levels of coulomb friction employed (0.05 and 0.25 lb-ft) are those bounding the expected range.

Figure 11a illustrates acquisition characteristics with minimum expected linkage friction and minimum expected structural damping. Effect of array flexibility is evident in the oscillatory traces of axis rates. The expanded scales may give a false impression; the oscillation amplitude is actually only a fraction of a degree per second, and cannot be seen in terms of array positions on the lower traces. A point to note is that the oscillation damps quite rapidly when the rate returns to zero – an indication of the significant effect of even this minimum amount of coulomb friction.

Figure 11b illustrates the effect of increasing the array structural damping to a value of 1 percent. Improvement in oscillatory characteristics is noticeable, although the maneuver is otherwise identical.

Figure 11c illustrates the pronounced effect of coulomb friction at its highest expected value, even with structural damping at the minimum. Although structural damping at off-zero rates is unaffected, coulomb damping tends to strongly squelch the initial kick as the arrays start moving (drum-axis particularly) so that the oscillation is initiated at lower amplitude.

It should be noted in all cases that evidence of oscillation in the motor torque traces, i.e., reaction into the vehicle, is at a negligible level.

Figure 12a illustrates noon-turn performance with minimum expected friction and damping. The problem was initiated with the vehicle about 6 degrees ahead of the sun line in-orbit position. Although steering error

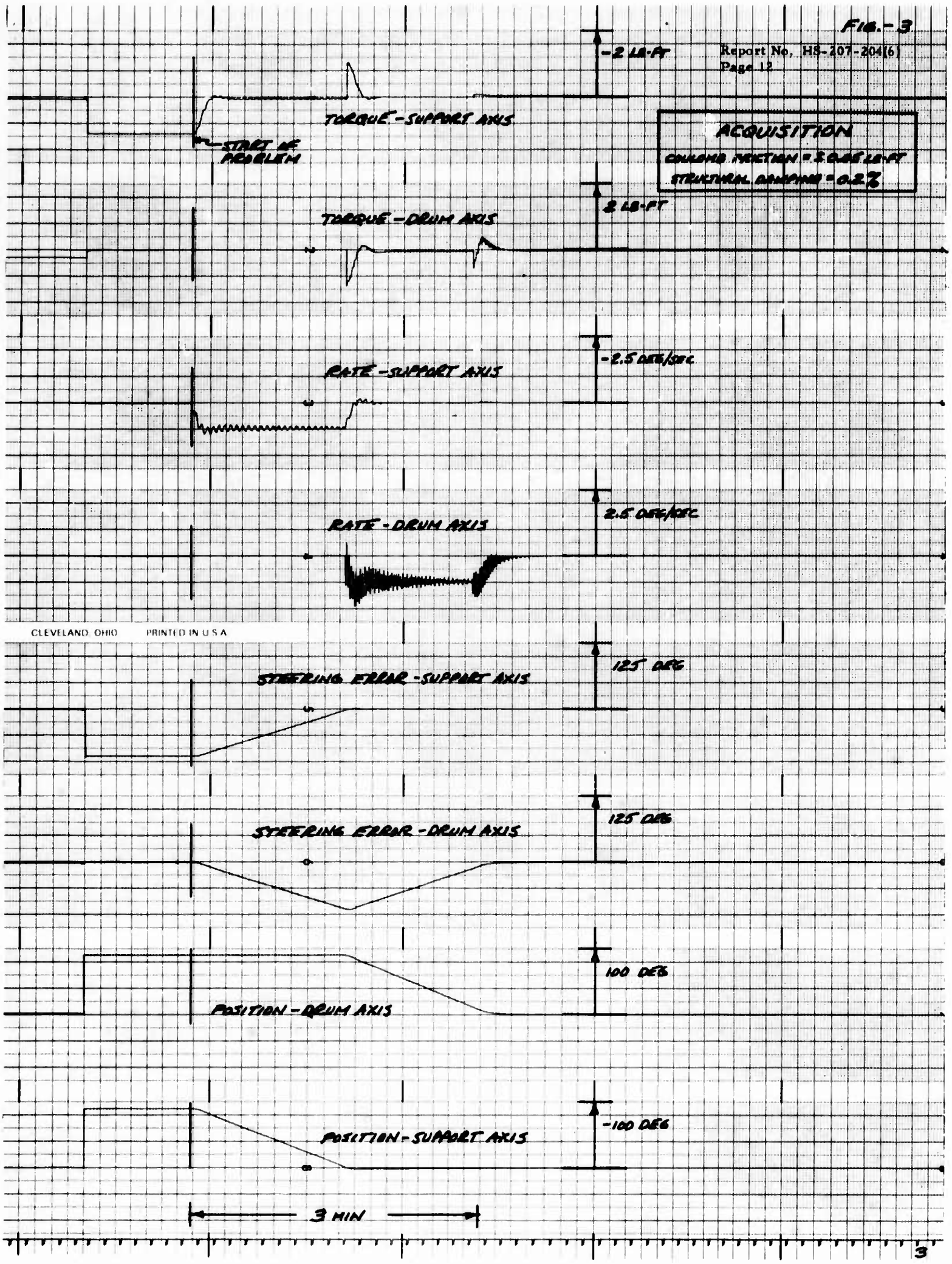

a) Coulomb Friction = ± 0.05 lb-ft
Structural Damping = 0.2 Percent

Figure 11. Performance in Sun Acquisition

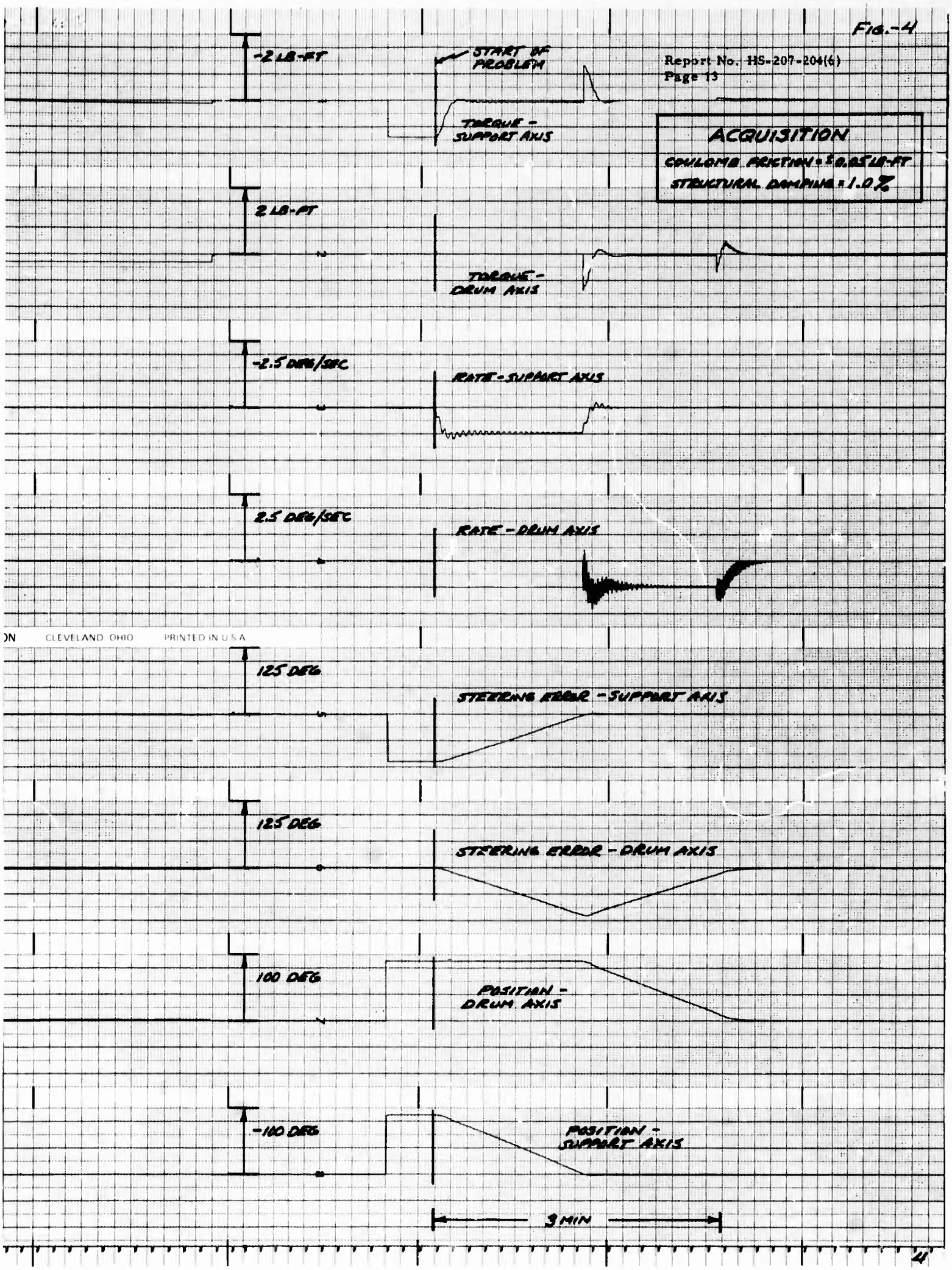

b) Coulomb Friction = ±0.05 lb-ft
Structural Damping = 1.0 Percent

Figure 11 (continued). Performance in Sun Acquisition

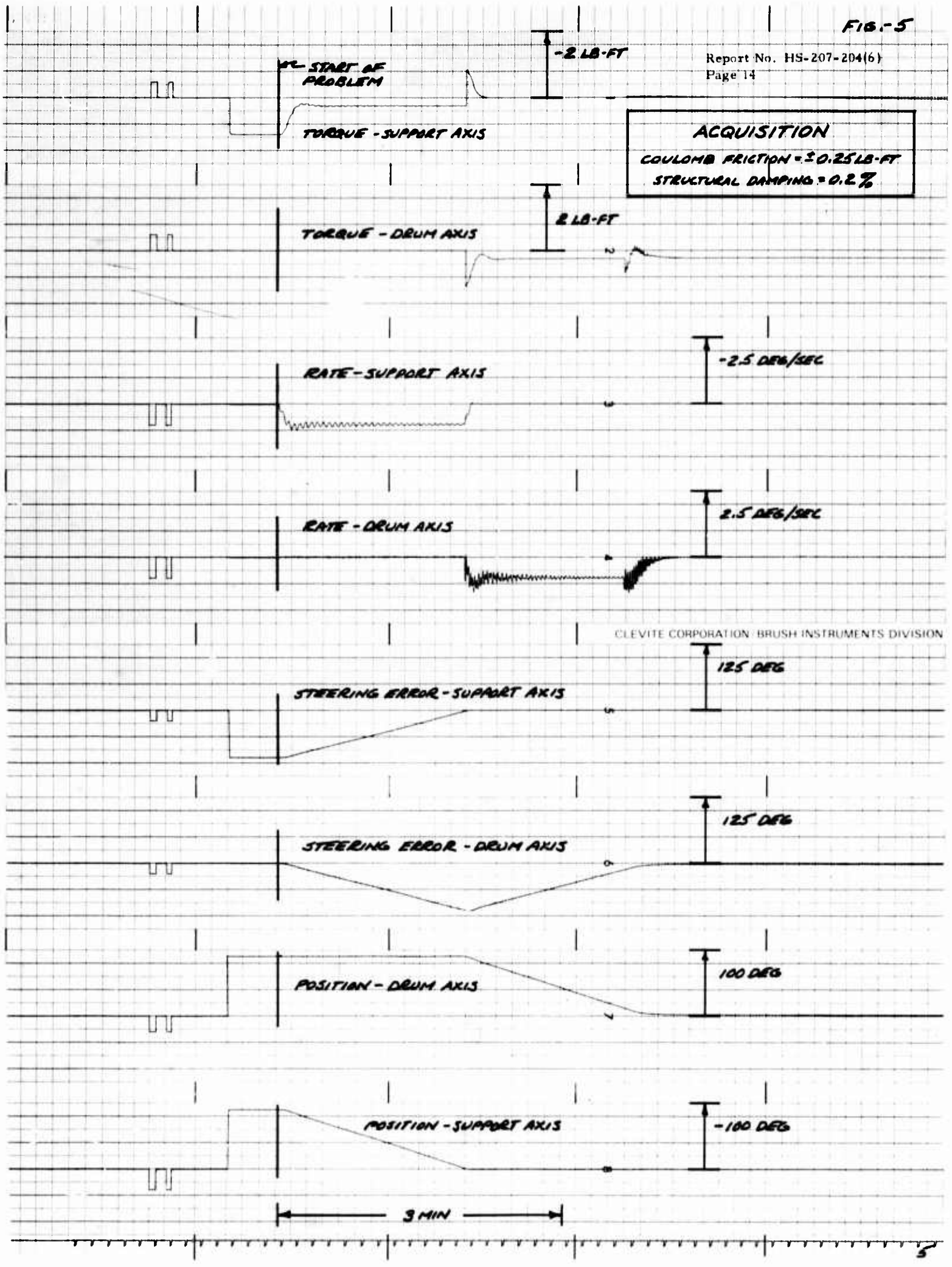

c) Coulomb Friction = ± 0.25 lb-ft
Structural Damping = 0.2 Percent

Figure 11 (continued). Performance in Sun Acquisition

and support-axis gain are low at this position, the friction is low enough so that the turn starts immediately. The turn is well-behaved, with a maximum array pointing error of 6 degrees.

Noon-turn performance with maximum expected linkage friction is indicated in Figure 12b. Here, the turn is delayed past the sun line, while the pointing-error-induced torque builds up to the friction value. The turn is then executed smoothly, with about a 20-degree maximum array-pointing error. Time in excess of 10 degrees is 110 seconds. This is insignificant in terms of gross electrical energy loss. (The slight buzz in drum-axis rate about the middle of the turn should be ignored; it is evidence of a minor equipment problem, not system performance.)

Controls Design Review

A review of the functional design of the linkage controls was held on April 16. Primary action items resulting from this review were:

1) To refine analysis to provide adequate confidence in loop stability with structural dynamics appropriately accounted for

2) To undertake work to provide a better definition of the level of array structural damping, including effects of friction in the boom-length compensator, storage drum, and cushion-reel roller

3) To refine the array-dynamics model to include structural cross-coupling and three-dimensional oscillations of the panel as a membrane

Effort deriving from item 1 has been incorporated in the results reported in the previous section. Hughes is now fully confident that the system is stable and the performance acceptable.

Items 2 and 3 represent work that should eventually be undertaken to firm up areas where data or dynamics are presently imperfectly understood or known only in a gross qualitative sense. Improved knowledge in these areas will allow much more precise determination of array dynamics. Hughes has had to design for worst-case conditions; whereas actual system damping may be much better than these conservative assumptions. Work in these areas would provide information for a more confident and efficient approach to the design of future larger array systems.

Control Electronics Unit

The control electronics unit design is essentially complete. The revised design incorporates the following minor changes:

1) In order to implement rate limiting in a gradual manner, a circuit incorporating a deadband followed by a gain characteristic as defined in Figure 9 is now employed.

FIG.-6

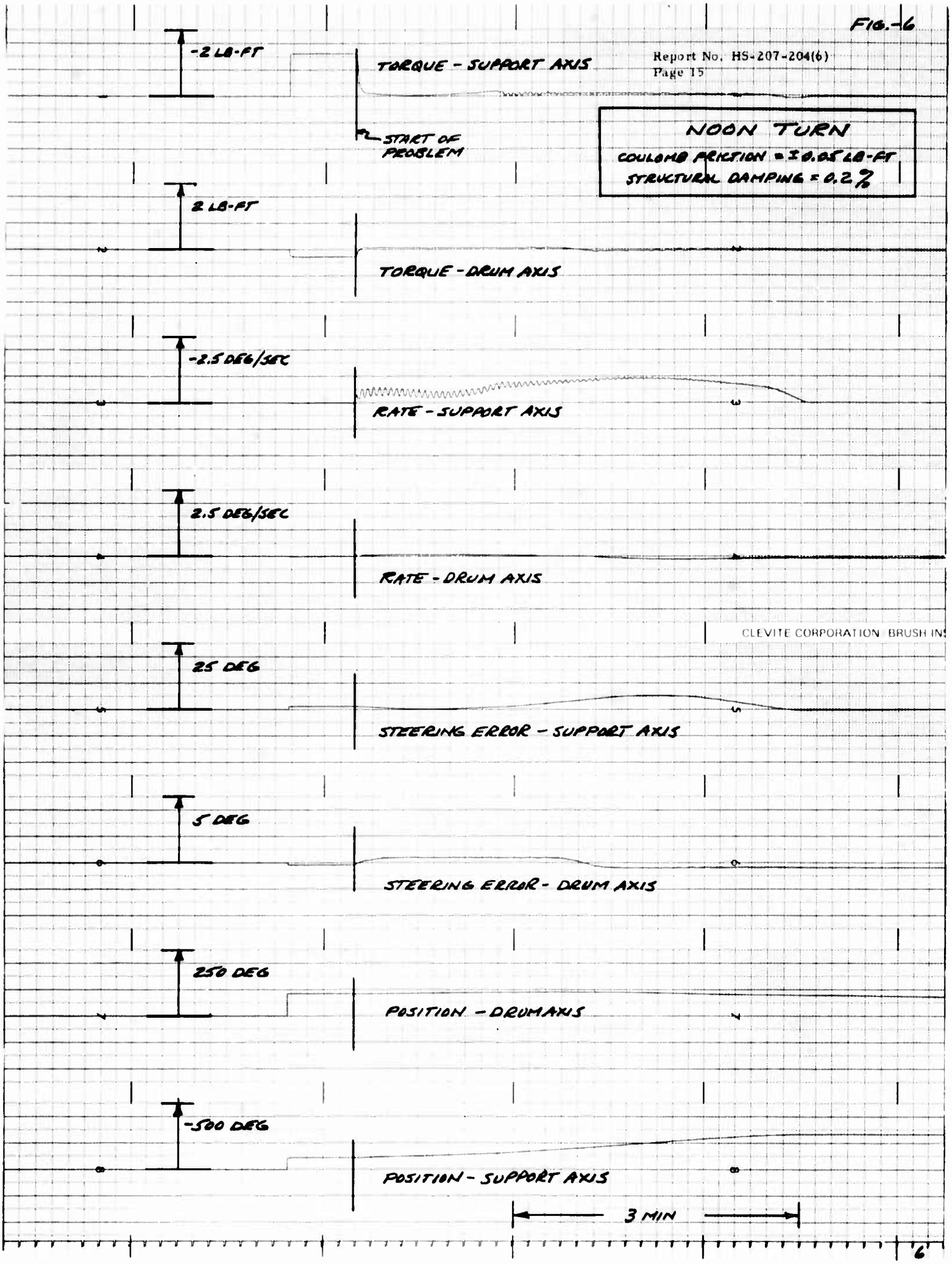

a) Coulomb Friction = ± 0.05 lb-ft
Structural Damping = 0.2 Percent

Figure 12. Performance in Noon Turns

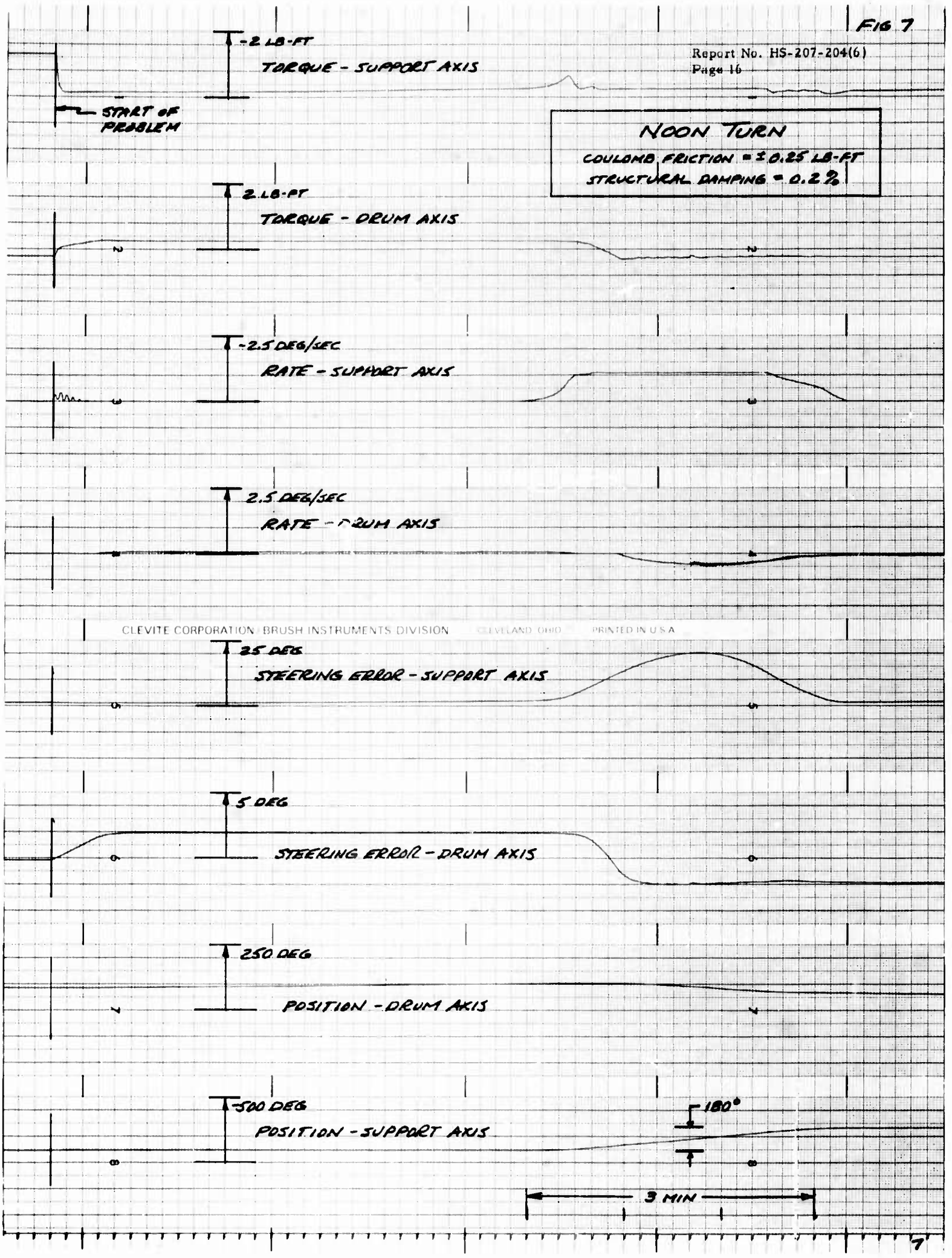

b) Coulomb Friction = ± 0.25 lb-ft
Structural Damping = 0.2 Percent

Figure 12 (continued). Performance in Noon Turns

2) Eclipse-mode logic is changed to allow elimination of the "sun-present" sensors. It is apparent that there is little difference in the CEU electrical load during eclipse between zero-torque and friction-torque levels of motor excitation. It is, therefore, feasible to start 1 deg/sec support-axis acquisition slew immediately upon entering eclipse; and it is then unnecessary to provide the special sensors for detecting emergence and restarting acquisition, as was previously done. A revised logic employing the tracking sensor cells is illustrated schematically in Figure 13. For either channel, with both cells dark, the resistance through the path is maximum, and the current minimum. Light on either cell will reduce resistance and raise the current above a selected detection threshold. The remaining logic provides the same functions as are presently incorporated.

3) Dual-range torque-motor current sensing and telemetry are incorporated. (Adds a 1-ampere range, as well as retaining the original 10-ampere range.)

4) Telemetry to indicate the state of the emergency-mode switches (right-hand side of mechanization diagram*) has been added.

5) In acquisition, the delay between the end of the support-axis drive phase and the start of the drum-axis drive phase were mechanized at 2 seconds. In order to better accomplish its purpose of preventing simultaneous large loads in both torquers, this lag was increased to 6 to 8 seconds.

Package design, which includes etched circuit board layouts and the structural housing design, is now under way. A complete drawing release is scheduled for 1 September.

MEETINGS

A presentation was prepared and given to a Symposium/Working Group (TTCP-M4) on Flexible Vehicle Dynamic Interactions, at Aerospace Corporation on May 20. The presentation covered three areas: 1) the details of the dynamics analysis of the FISCA boom/panel structure, 2) the design and performance of the orientation linkage control loop including the effects of array flexibility, and 3) the models, techniques, and tools associated with the evaluation of the interactions between the array control system, array flexibility, and the vehicle control system. The presentation was well-received and discussions with other members of the Working Group indicated that the subject of flexibility has been pursued in substantial depth on the LRSCA project.

---

*Third Quarterly Report.

On June 17, Controls personnel participated in the first of a number of meetings to be held with the integrating contractor, LMSC. This meeting was devoted to a review of drawings and material in the present interface specification. Later meetings are expected to explore the subject of dynamic interactions between the arrays, linkage controls, and vehicle in greater detail.

PLANS FOR NEXT QUARTER

Effort during the coming quarter will be devoted to the following items:

1) Completion of drawing check and stress analysis

2) Fabrication and beginning the testing of the orientation mechanism development test model

3) Completion of the ECU design drawings, and start of fabrication of the qualification unit

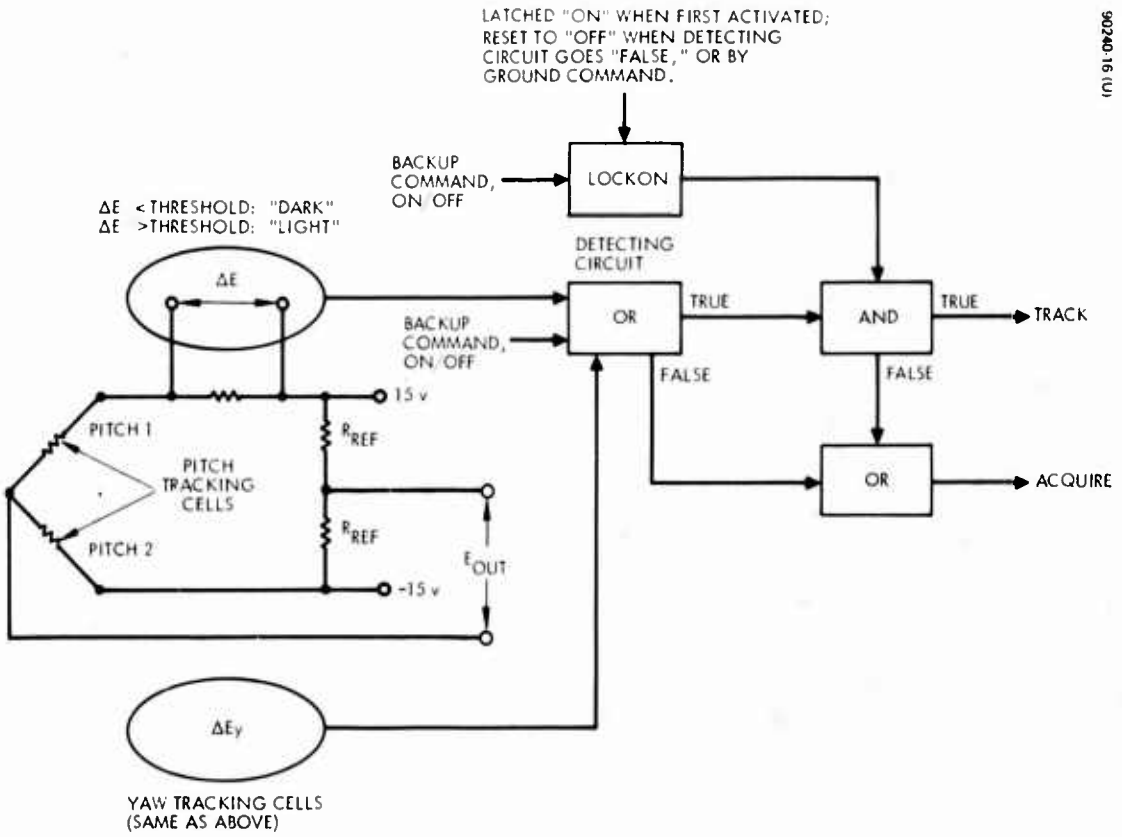

Figure 13. Acquire/Track Logic

SECTION VI

POWER SUBSYSTEM

SUMMARY

The battery charging techniques have been refined to simplify the associated electronics. The new technique has been verified by laboratory testing. The overvoltage-undervoltage sensing circuit and the battery charger are presently in the breadboard stage. The voltage regulator test load bank, inverter, and motor control are in the design stage and will be breadboarded during the next quarter. Specific detail of the work accomplished is presented below.

BATTERY CHARGE CONSIDERATIONS

In order to simplify the electronics design, the tolerances associated with the battery charging scheme have been relaxed. Previously, two levels of charge were utilized with the charge rate beginning at 1.0 ± 0.5 ampere until the cell voltage reaches 1.46 ± 0.01 volts. At this point, the charge current was to be reduced to 0.60 ± 0.03 ampere. It returned to the 1.0 ± 0.05 ampere rate when the cell voltage dropped to 1.28 ± 0.02 volts. To maintain energy balance, i.e., assure that sufficient recharge is returned to the batteries each orbit, the charge current must be maintained at the higher rate of 1.0 ampere for a specific portion of the charging time depending on temperatures. This portion of time is temperature-dependent because the charge acceptance of the batteries is a function of temperature.

Table IV gives the required charge time, as a function of temperature, before switching from 1.0 to 0.6 ampere. Charge time is expressed as a percentage of the minimum sunlight portion per orbit (53 minutes).

TABLE IV. CHARGE TIME AS FUNCTION OF TEMPERATURE

Temperature, ° F	Percent of Charge Time at 1.0 Ampere
40	10.2
60	37.6
80	60.0
90	100.0

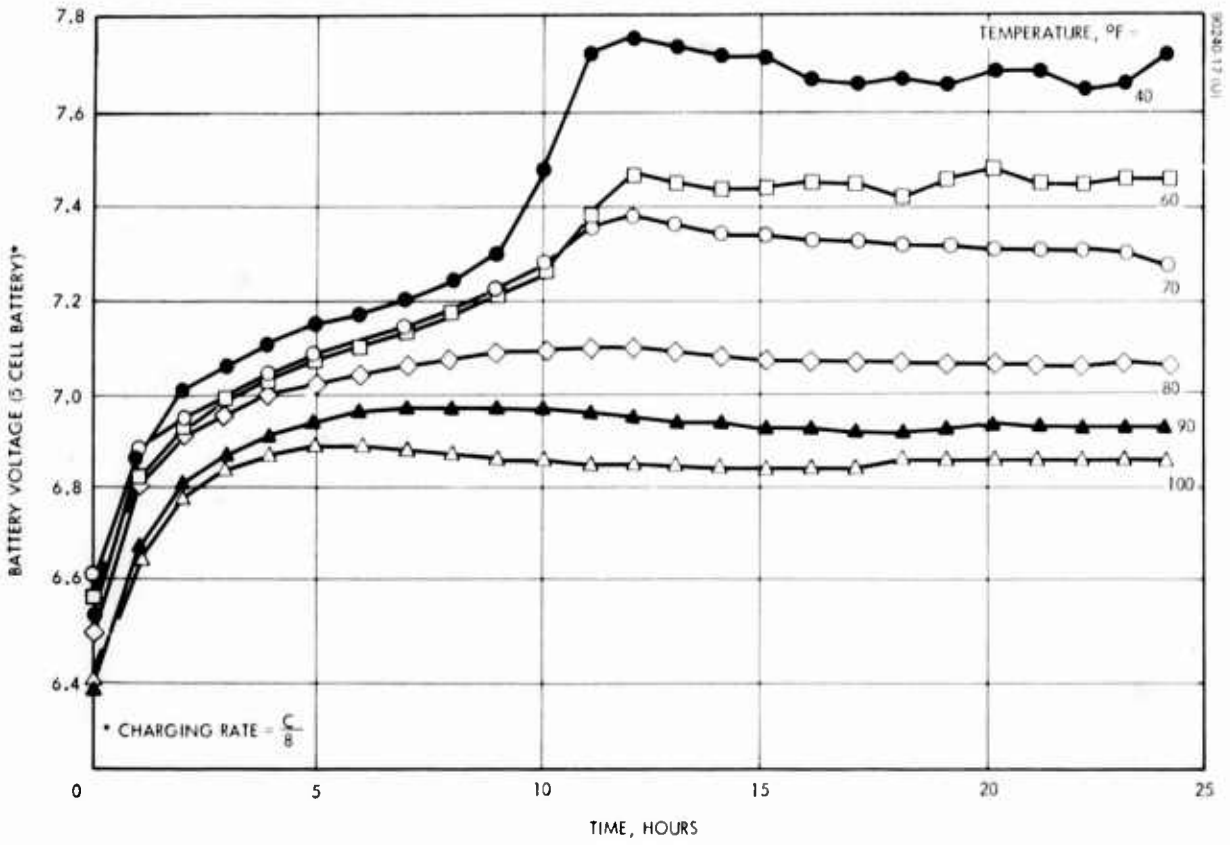

Figure 14. Nickel Cadmium Battery Charge Characteristics at Various Temperatures

The overcharge rate the batteries will tolerate without experiencing excessive internal oxygen pressure buildup is a function of temperature. This design is based on a battery cell configuration that will tolerate an overcharge rate of 1.0 ampere above 70° F and 0.6 ampere below 70° F.

To avoid overcharging at the 1.0 ampere rate at temperatures below 70° F. cell voltage is sensed and the current reduced from 1.0 ampere when the cell voltage increases to a nominal value of 1.45 volts. It is characteristic of these cells that the voltage rises above 1.45 volts as full charge is approached, provided the temperature is below 70° F. Typical charge curves indicating this characteristic are shown in Figure 14.

The set point of 1.45 volts must be maintained within the tolerances shown below, i.e., at 70° F, within 0.01 volt. If the set point tolerance were relaxed upward, for example to +0.04 volt, no cutback might occur at a temperature of 60° F. The battery would thus enter overcharge at the high rate, which violates the criterion of not overcharging at the high rate below 70° F.

On the other hand, if the set point tolerance were relaxed downward to -0.04 volt, cutback might occur prematurely. For example, cutback would occur after attaining 50 percent state of charge at 80° F, resulting in an out of energy balance condition since the high rate charge must be maintained for 60 percent or more of the time at this temperature.

To avoid excessive electronic complexity and resulting unreliability, it is desirable that the tolerance be as wide as possible. Two steps are being taken, as follows:

1) Locating the charge controller thermally adjacent to its battery

2) Establishing the tolerance, as follows:

Temperature, ° F	Set Point, volts
40	1.45 + 0.02 - 0.01
70	1.45 + 0.01 - 0.01
90	1.45 + 0.01 - 0.03

This approach permits the system to operate as planned and does not require sophisticated electronics design. The overall set point tolerance is +0.02 - 0.03 over the temperature range. The electronics breadboard test results obtained this quarter are well within these specified set point values.

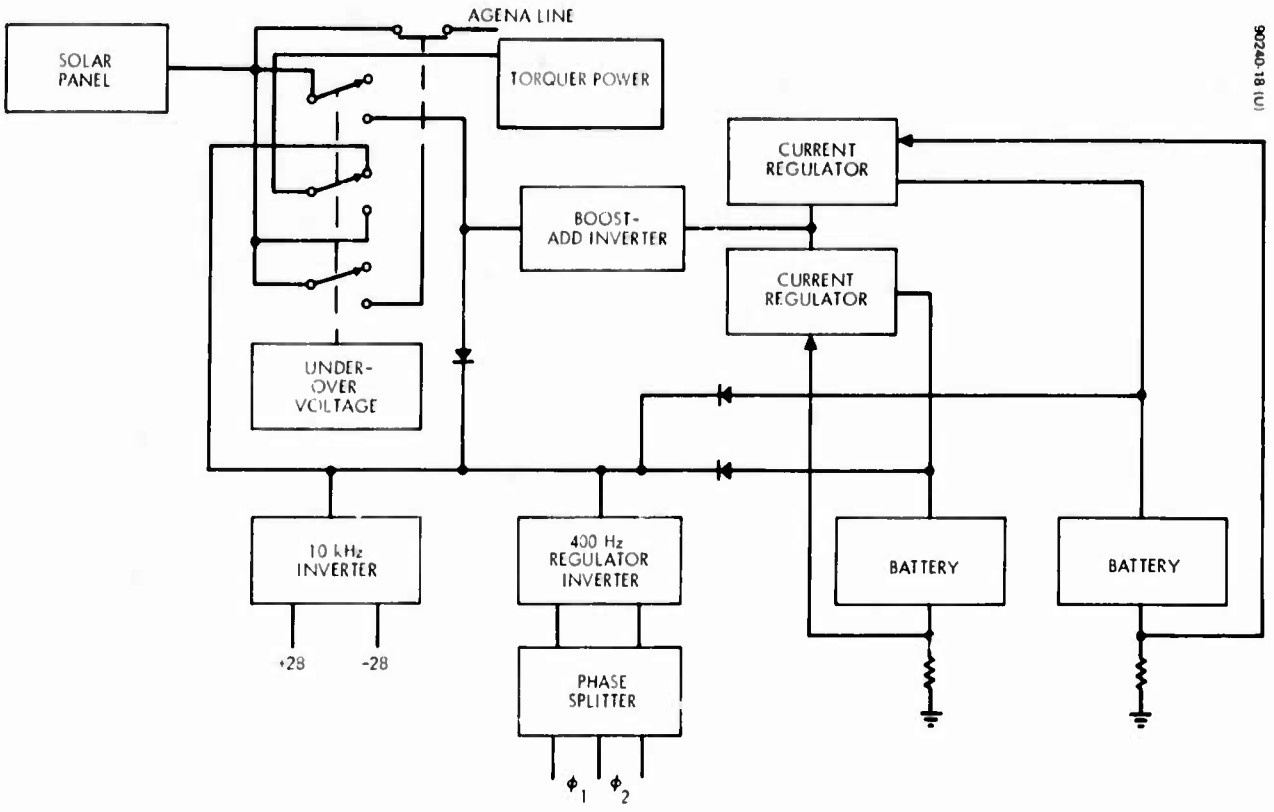

Figure 15. Block Diagram of Power Subsystem

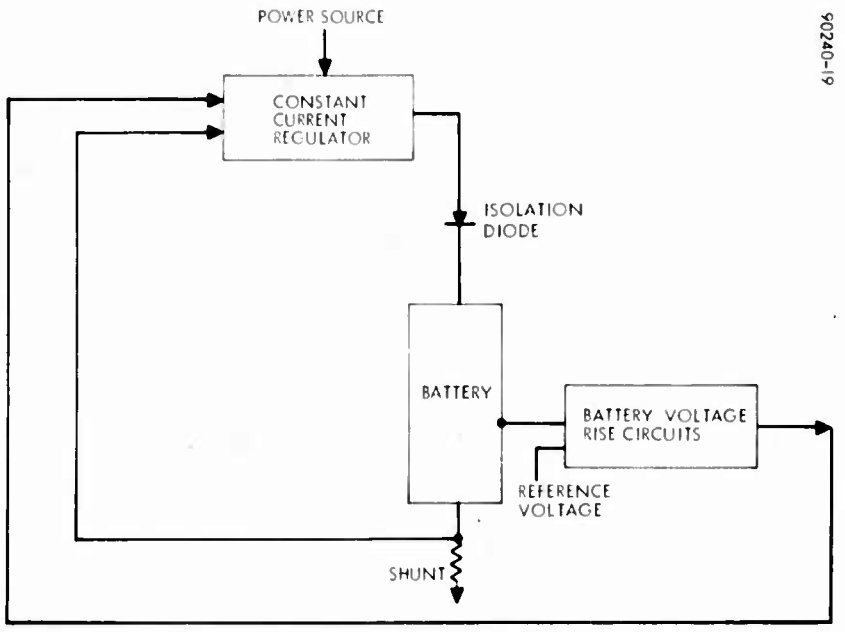

Figure 16. Block Diagram of Battery Voltage Rise and Constant Current Charge Circuits

POWER CONDITIONING ELECTRONICS

A study of the possible circuit combinations for power conditioning was completed. The output requirements are regulated +28 volts dc, regulated -28 volts dc, constant current for battery charging and two-phase 400 Hz power for the extend/retract motor. The study compared circuits with input or output regulation and power conversion at 10 kHz for all but motor power.

The preferred system is shown in Figure 15.

The power conditioning unit utilizes an undervoltage-overvoltage circuit that disconnects the solar panel bus from its load when the solar panel output voltage is at a dangerously high level or is too low to properly support the load. Upon emergence from an eclipse, it senses the open circuit voltage of the panel and closes the solar panel switch after the panel becomes warm and the panel voltage has decreased to a safe operating value. This value had been tentatively set at 36 volts. With a clearer definition of the electrical and thermal characteristics of the solar panel for a 400 n.mi. orbit, its 36-volt overvoltage setting was found to be inadequate; accordingly, this value has been increased to 43 ± 1 volts to ensure that the solar panel is supplying power to the bus for the maximum length of time feasible. Similarly, the undervoltage setting has been reduced from 23 volts to 21 ± 1 volts. Changes to the power conditioning electronics as a result of the wider voltage range are being incorporated.

A preliminary design review for the power conditioning unit and the battery was held on 2 May 1969. The basic design concepts as described were evaluated and accepted.

BATTERY CHARGE CONTROLLER BREADBOARD TESTS

The battery voltage rise circuit senses the potential across one of the battery cells during charge and sends a digital signal to the constant current regulator. If the voltage across the battery cell is below a selected voltage level, the charge current is in the high state. When cell potential exceeds the selected voltage level, the charge current automatically switches to the low state. This circuit is shown in Figure 16. The test setup is shown in Figure 17.

Results of temperature tests on the battery voltage rise switch and constant current charge circuit are listed in Table V.

The voltage rise switch set point varied by ±18 millivolts over the temperature range of -5° to 160° F. The voltage rise switch set point decreased as temperature increased. The data presented in Table V indicate operating characteristics that are within the set point tolerances established, even at temperatures significantly beyond the design temperature range.

TABLE V. BATTERY VOLTAGE RISE AND CONSTANT CURRENT CHARGE CIRCUIT TEST SUMMARY

Test Temperature, °F	High Charging Rate	Cell Voltage Set Point, volts	Low Charging Rate	Cell Voltage After Cut-back, volts
74	1.005	1.450	0.580	1.301
74	1.005	1.450	0.580	1.301
-5	1.025	1.455	0.600	1.315
-5	1.026	1.456	0.600	1.314
-5	1.030	1.456	0.600	1.316
-5	1.030	1.455	0.600	1.316
154	0.985	1.422	0.580	1.303
156	0.985	1.422	0.580	1.304
160	0.980	1.422	0.580	1.299
160	0.980	1.423	0.580	1.300

Figure 17. Temperature Test Setup of Battery Charge Controller

(Photo A24322)

SECTION VII

INSTRUMENTATION SUBSYSTEM

PURPOSE AND GENERAL REQUIREMENTS

The primary purpose of the instrumentation subsystem is to obtain data from the LRSCA experiment to evaluate its performance during flight and test. A variety of sensors and associated conditioning circuitry are provided to obtain these data. Instrumentation signals from the solar array and orientation linkage are conditioned to a 0 to +5 volt format, multiplexed in pulse amplitude modulation (PAM) commutators, and applied to the Agena telemetry subsystem for further signal processing. Instrumentation signals associated with the power conditioning and storage subsystem are conditioned to a 0 to +5 volt format and applied directly to the Agena telemetry commutator. The subsystem is designed to be compatible with the Air Force Space-Ground Link Subsystem (SGLS).

NEW MEASUREMENTS

New measurements have been added to the orientation linkage and power conditioning and storage subsystems. The revised lists are shown in Tables VI and VII.

New measurements are also being added to the solar array subsystem. Three accelerometers and a strain gauge amplifier are being mounted on the boom tips of array panel 2 to match the data being obtained from array panel 1. Two accelerometers are being added to the inboard boom actuator. Fourteen reference solar cells and solar cell modules are being added to both solar panels to obtain comparison V-I curves. The reference cell and module electronics is described below.

REFERENCE SOLAR CELL AND MODULE SIGNAL PROCESSOR ELECTRONICS

The solar cell signal processing electronics is being incorporated into the LRSCA experiment on a minimum interference basis. Each individual signal will be conditioned to a 0 to +5 volt format and then commutated prior to application to the launch vehicle telemetry subsystem through a drum-axis and a support-axis slipring. The new commutator will be identical to the two 45-word four-frame/second PAM commutators presently being used.

Figure 18 is a functional block diagram of the processing electronics. Solar cell selection and loading are controlled by miniature relays.

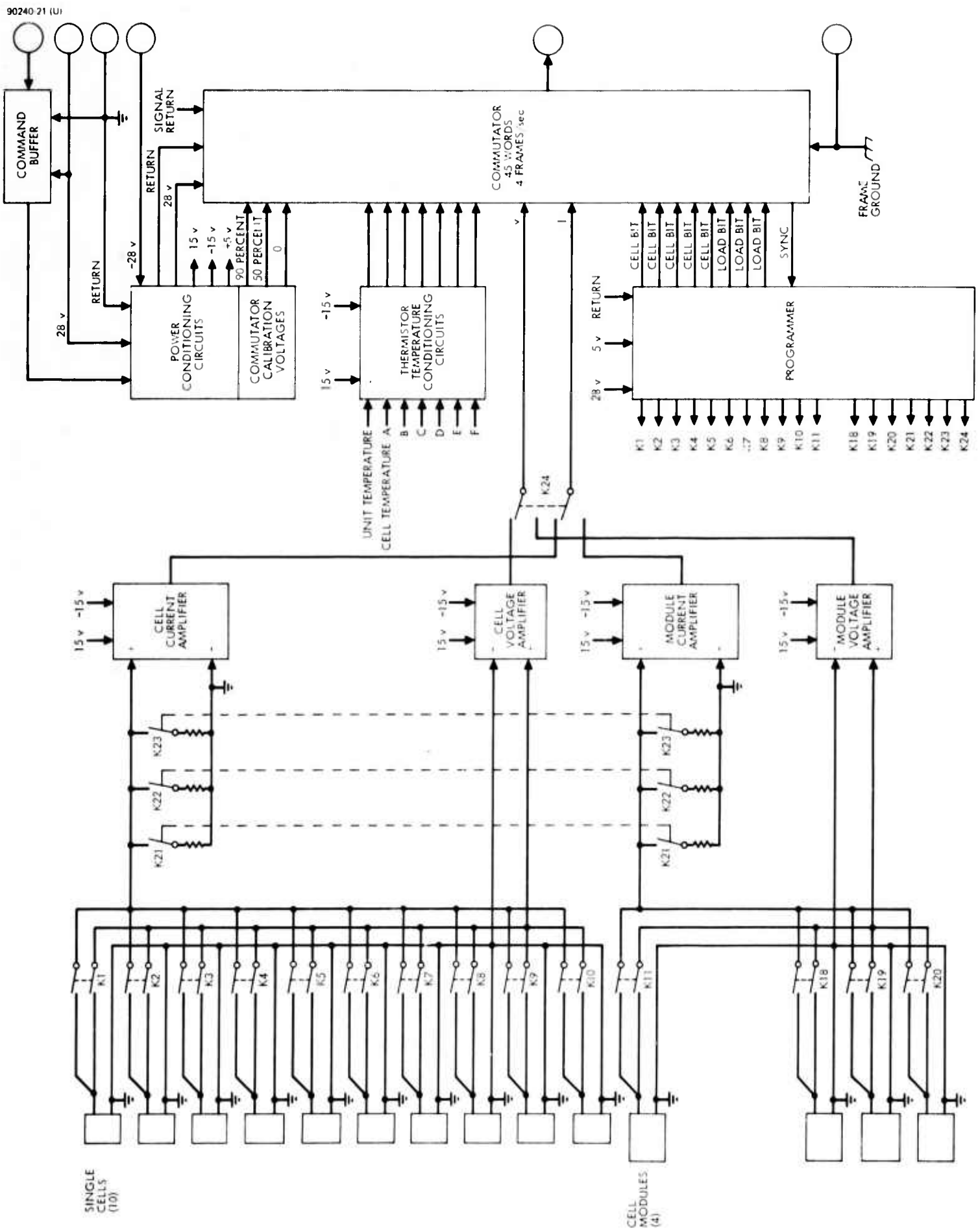

Figure 18. Reference Solar Cell and Solar Cell Module Circuit Diagram

TABLE VI. ORIENTATION LINKAGE COMMUTATOR TELEMETRY MEASUREMENTS

Data Channel	Function
B-1	Zero calibration
B-2	Full-scale calibration
B-3	Sun present signal
B-4	Acquisition sensor, positive
B-5	Acquisition sensor, negative
B-6	Tracking sensor, lockon cell
B-7	Tracking sensor, drum axis error
B-8	Tracking sensor, support axis error
B-9	Sun sensor excitation, +15 volts dc
B-10	Sun sensor excitation, -15 volts dc
B-11	Drum axis torquer current (high level)
B-12	Support axis torquer current (high level)
B-13	Control electronics unit, +5 volts dc
B-14	Control electronics unit, +28 volts dc
B-15	Control electronics unit, -28 volts dc
B-16	Solar array subassembly deployed and locked
B-17	Drum axis tachometer voltage
B-18	Support axis tachometer voltage
B-19	Drum axis torquer temperature
B-20	Support axis torquer temperature
B-21	Drum axis tachometer temperature
B-22	Support axis tachometer temperature
B-23	Control electronics unit temperature A

Table VI (continued)

Data Channel	Function
B-24	Control electronics unit temperature B
B-25	Control electronics unit temperature C
B-26	Control electronics unit temperature D
B-27	Drum axis structure temperature
B-28	Drum axis brush temperature
B-29	Drum axis bearing temperature
B-30	Support axis structure temperature
B-31	Support axis brush temperature
B-32	Support axis bearing temperature
B-33	Torquer voltage
B-34	Drum axis torquer current (low level)
B-35	Support axis torquer current (low level)
B-36	Manual torque drum axis negative
B-37	Manual torque drum axis positive
B-38	Manual torque support axis negative
B-39	Manual torque support axis positive
B-40	Torquer drive AUTO
B-41	Manual sun lockon
B-42	Limit override
B-43	Manual sun present
B-44	Synchronization
B-45	Synchronization

TABLE VII. POWER CONDITIONING UNIT TELEMETRY MEASUREMENTS

Data Channel	Function
C-1	LRSCA unregulated voltage
C-2	Battery 1 voltage
C-3	Battery 2 voltage
C-4	Battery 1 charge current
C-5	Battery 2 charge current
C-6	Regulated voltage (+28 volts)
C-7	Regulated voltage (-28 volts)
C-8	Regulated current (+28 volts)
C-9	Regulated current (-28 volts)
C-10	Solar array motor current
C-11	Inverter A voltage
C-12	Inverter B voltage
C-13	Input regulator output voltage
C-14	Battery 1A temperature
C-15	Battery 1B temperature
C-16	Battery 1C temperature
C-17	Battery 1D temperature
C-18	Battery 2A temperature
C-19	Battery 2B temperature
C-20	Battery 2C temperature
C-21	Battery 2D temperature
C-22	Power conditioning unit temperature
C-23	Battery 1 discharge current
C-24	Battery 2 discharge current
C-25	Spare
C-26	Spare
C-27	Spare

Three precision (0.1 percent) resistive loads are switched sequentially, providing a total of eight load combinations. There are ten cell measurements and four module (consisting of eight series by three parallel cells) measurements that require two sets of loads switched by separate contacts of a common relay.

After one of the eight loads (including open circuit) has been selected, all 14 cells and modules are sequentially switched in for a period of 1 second each. During this 1-second time period, all measurements are read out four times. After all 14 cell and module voltage, current, and temperature measurements have been completed for a selected load condition, the next load is selected, and the above scanning sequence is repeated.

Current for each load condition is determined by measuring the voltage drop across the precision load resistors. This voltage is then amplified to a 0 to +5 volt format prior to application to the commutator.

Voltages are measured directly across the cell or module terminals to compensate for the harness drop. This voltage is also amplified up to the 0 to +5 volt level prior to commutation.

The programmer controls the turnon and turnoff of the load, current, and voltage relays. It also provides four digital bits that indicate which cell or module is currently selected plus three digital bits that indicate the load condition. These seven digital bits are telemetered to earth along with the other measurements. A frame sync-pulse (four per second) from the commutator is employed as a clock pulse for the programmer.

Seven thermistor temperature measurements are processed in the electronics units also (six panel and one internal electronics unit measurements). These utilize the precision 15-volt supply and voltage divider networks in a manner identical to the other LRSCA temperature measurements.

The signal processor circuits require +28, +15, -15, and +5 volts. These voltage levels are derived in the power conditioning section from +28 volts and -28 volts supplied from the power conditioning unit on the orbital equipment rack. A ground command will apply and remove power from the signal processor electronics and the commutator. I-V curves of the cells and module will only be taken during specified station visibility periods to prevent needless, continuous cycling of the relays.

The solar cell electronics unit and the new commutator will be mounted on the outboard boom actuator.

SOLAR ARRAY COMMUTATOR SIGNALS

The signals that will be processed by the new solar array commutator 2 are listed in Table VIII. Since the accelerometers and strain gauge signals are supercommutated to increase their sample rate to 12 per second, they appear in the table three times (frame rate is four per second).

DELETED MEASUREMENTS

The sun present sensors have been deleted from the LRSCA experiment, and therefore these measurements have been deleted from the solar array commutator 1 list of measurements. The current list is shown in Table IX.

INSTRUMENTATION CONDITIONING UNIT

Elimination of the sun present sensors has resulted in changes to the instrumentation conditioning unit (ICU). The old sun present circuitry has been removed and replaced by two operational amplifiers that sense the current through the drum-axis and support-axis cells of the tracking sensor. The two amplifier outputs are combined in an OR gate and provide a sun present signal to the control electronics unit (CEU). The new circuitry has been incorporated into the breadboard developmental model.

PROCUREMENT SPECIFICATIONS

The commutators, accelerometers, and strain gauge amplifiers procurement specifications have been completed and reviewed by the vendors.

WORK TO BE PERFORMED DURING NEXT REPORTING PERIOD

The following will be performed during the fifth quarter:

1) Complete thermal study for all instrumentation subsystem control items

2) Complete developmental model testing of new ICU sun sensor circuitry

3) Continue product design of ICU

4) Develop detail design requirements for solar cell electronics

5) Initiate circuit design of solar cell electronics

TABLE VIII. SOLAR ARRAY COMMUTATOR 2
TELEMETRY MEASUREMENTS

Data Channel	Function
D-1	Zero calibration
D-2	Full-scale calibration
D-3	Midscale calibration
D-4	STEM tip inboard accelerometer (V-axis)
D-5	STEM tip inboard accelerometer (U-axis)
D-6	STEM tip outboard accelerometer (V-axis)
D-7	STEM tip outboard accelerometer (W-axis)
D-8	Drum mechanism inboard accelerometer (V-axis)
D-9	Boom length compensator strain gauge
D-10	Cell/module selection 1
D-11	Cell/module selection 2
D-12	Cell/module selection 3
D-13	Cell/module selection 4
D-14	Spare
D-15	Load condition 1
D-16	Load condition 2
D-17	Load condition 3
D-18	Spare
D-19	STEM tip inboard accelerometer (V-axis)
D-20	STEM tip inboard accelerometer (U-axis)
D-21	STEM tip outboard accelerometer (V-axis)
D-22	STEM tip outboard accelerometer (W-axis)
D-23	Drum mechanism inboard accelerometer (V-axis)

Table VIII (continued)

Data Channel	Function
D-24	Boom length compensator strain gauge
D-25	Solar cell electronics temperature
D-26	Array panel 1 temperature
D-27	Array panel 1 temperature
D-28	Array panel 1 temperature
D-29	Array panel 2 temperature
D-30	Array panel 2 temperature
D-31	Array panel 2 temperature
D-32	Cell/module voltage
D-33	Cell/module current
D-34	STEM tip inboard accelerometer (V-axis)
D-35	STEM tip inboard accelerometer (U-axis)
D-36	STEM tip outboard accelerometer (V-axis)
D-37	STEM tip outboard accelerometer (W-axis)
D-38	Drum mechanism inboard accelerometer (V-axis)
D-39	Boom length compensator strain gauge
D-40	Solar cell electronics ON/OFF
D-41	Spare
D-42	Spare
D-43	Spare
D-44	Synchronization
D-45	Synchronization

Note: All tip-mounted accelerometers and strain gauges on this commutator channel are located on array panel 2.

TABLE IX. SOLAR ARRAY COMMUTATOR 1
TELEMETRY MEASUREMENTS

Data Channel	Function
A-1	Zero calibration
A-2	Full-scale calibration
A-3	STEM tip inboard accelerometer (V-axis)
A-4	STEM tip outboard accelerometer (W-axis)
A-5	STEM tip outboard accelerometer (V-axis)
A-6	Drum mechanism accelerometer (V-axis)
A-7	Drum mechanism accelerometer (W-axis)
A-8	Boom length compensator strain gauge
A-9	STEM strain gauge
A-10	Solar array motor temperature
A-11	Solar array voltage
A-12	Array position indicator (pulse count)
A-13	Spreader bar temperature
A-14	Solar array fully extended
A-15	Solar array fully retracted
A-16	Solar panel temperature A
A-17	Solar panel temperature B
A-18	STEM tip inboard accelerometer (V-axis)
A-19	STEM tip outboard accelerometer (W-axis)
A-20	STEM tip outboard accelerometer (V-axis)
A-21	Drum mechanism accelerometer (V-axis)
A-22	Drum mechanism accelerometer (W-axis)

Table IX (continued)

Data Channel	Function
A-23	Boom length compensator strain gauge
A-24	STEM strain gauge
A-25	Spare
A-26	Spare
A-27	Spare
A-28	Spare
A-29	Spare
A-30	Spare
A-31	Spare
A-32	Spare
A-33	STEM tip inboard accelerometer (V-axis)
A-34	STEM tip outboard accelerometer (W-axis)
A-35	STEM tip outboard accelerometer (V-axis)
A-36	Drum mechanism accelerometer (V-axis)
A-37	Drum mechanism accelerometer (W-axis)
A-38	Boom length compensator strain gauge
A-39	STEM strain gauge
A-40	Solar array subassembly released
A-41	Solar array 1 current
A-42	Solar array 2 current
A-43	Spare
A-44	Synchronization
A-45	Synchronization

Note: All tip-mounted accelerometers and strain gauges on this commutator are located on array panel 1. The drum-mounted accelerometers are located inboard.

SECTION VIII

SYSTEM TEST

Progress in the area of system test for this report period consists of:

1) Development of initial concepts and sketches of the LRSCA test fixture required for use with the water tables

2) Initial work with and exercise of the FISCA feasibility model in verifying and adjusting the preliminary water table setup

WATER TABLES

To facilitate the extension and retraction of the full-size solar panels, low-friction water tables have been fabricated. The test setup will consist of two large tables placed on each side of the solar panel drum (see Figure 19). The tables will provide a water surface approximately 1.5 inches deep upon which the panels will be floated, and will be large enough to accommodate the complete system in the deployed condition. The drum mechanism will be mounted between the pair of tables so that each panel will slide out over the table, supported at intervals on foam floats.

Status

The test area setup is complete. The sump-pump drain system is installed, and all but the final plumbing connections are complete. A temporary pedestal has been utilized for operations with the FISCA feasibility model. The feasibility model was received on loan from the Air Force Aero Propulsion Laboratory, Wright-Patterson Air Force Base, for initial checkout of the water table setup and for developing operating techniques.

The design of the foam floats and the test fixture are complete and negotiations are under way for fabricating same. The foam floats will be fabricated from Uthane 200 foam.

The overhead camera installation is in process. Special supports are required above the area's false ceiling for both the camera support and the solar array drum support.

PLANNED ACTIVITIES

Activities planned for the next reporting period include:

1) Procurement of the flotation blocks

2) Fabrication of the LRSCA test fixture

3) Installation of the necessary overhead girder reinforcement

4) Continued operation of the FISCA feasibility model for technique development

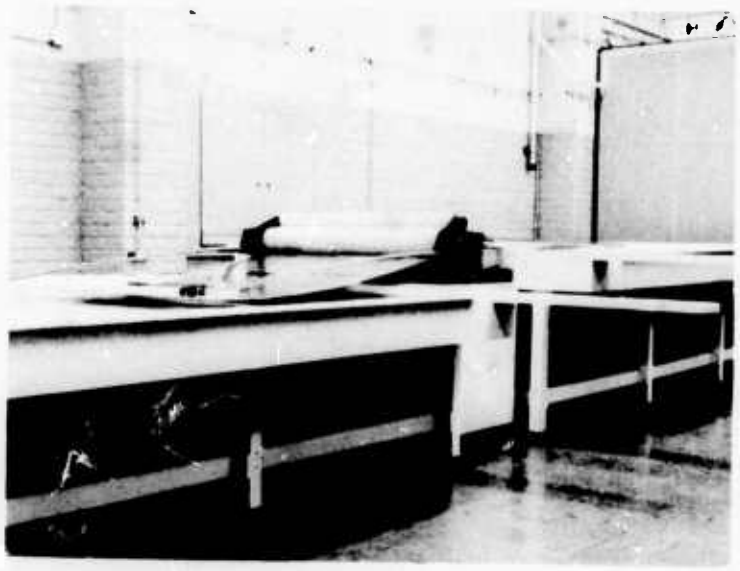

a) Side View
(Photo A24275)

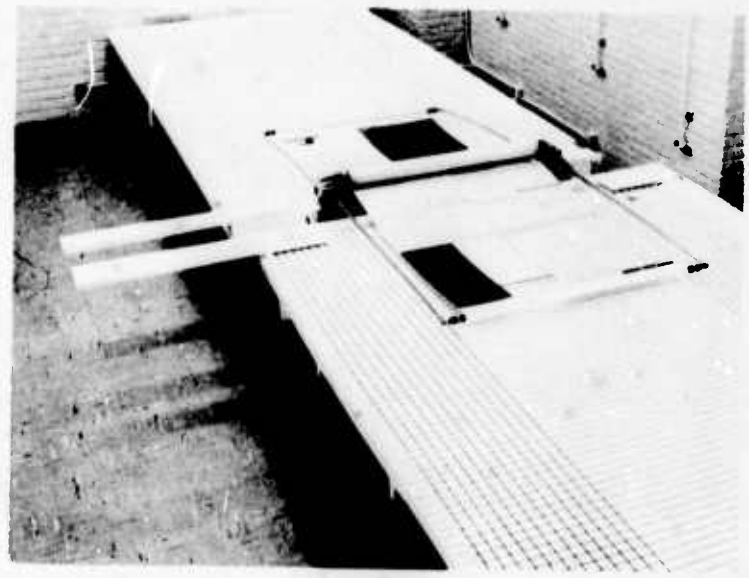

b) Top View
(Photo A24276)

Figure 19. Low-Friction Water Tables

SECTION IX

RELIABILITY

Life testing of components was initiated during the fourth quarter. The negator spring, a component of the drum mechanism which is used to control panel tension, was operated until a crack appeared after 4450 cycles.

The operating requirement of the negators during the LRSCA ground and flight test is 35 cycles. The probability that this requirement will be met can be calculated from the formula

$$R = \frac{n + 1}{n' + n + 1}$$

where n = number of operations before failure and n' is the required number of operations.

R therefore is:

$$\frac{4450 + 1}{35 + 4450 + 1} = 0.9922$$

This compares favorably with the previously apportioned number of 0.9900.

Extension tests were performed on a boom at Spar Aerospace. The boom was extended and retracted 314 times without anomalies.

As the program progresses and more hardware becomes available, additional reliability testing will be performed to verify that the previously apportioned numbers will be met or exceeded.

During the next quarter, the Preferred Parts List of electronic parts, as well as the system reliability and maintainability prediction, will be revised and updated.

UNCLASSIFIED
Security Classification

DOCUMENT CONTROL DATA - R & D

(Security classification of title, body of abstract and indexing annotation must be entered when the overall report is classified)

1. ORIGINATING ACTIVITY *(Corporate author)*
Hughes Aircraft Company
Space Systems Division
El Segundo, California

2a. REPORT SECURITY CLASSIFICATION
UNCLASSIFIED

2b. GROUP
Not Applicable

3. REPORT TITLE
Fourth Quarterly Technical Progress Report - Large Retractable Solar Cell Array

4. DESCRIPTIVE NOTES *(Type of report and inclusive dates)* Fourth Quarterly Technical Report;
24 March to 29 June, 1969

5. AUTHOR(S) *(First name, middle initial, last name)*
George Wolff
Edward O. Felkel

6. REPORT DATE	7a. TOTAL NO. OF PAGES	7b. NO. OF REFS
July 1969	58 printed	None

8a. CONTRACT OR GRANT NO.	9a. ORIGINATOR'S REPORT NUMBER(S)
F33615-68-C-1676	
b. PROJECT NO. 682J	69(22)-4490/B3532-006
c.	9b. OTHER REPORT NO(S) *(Any other numbers that may be assigned this report)*
d.	SSD 90240R

10. DISTRIBUTION STATEMENT
DDC
Cameron Station
Alexandria, Virginia 22314

11. SUPPLEMENTARY NOTES	12. SPONSORING MILITARY ACTIVITY
Not applicable	Air Force Aero Propulsion Laboratory APIP-2 Wright-Patterson AFB, Ohio 45433

13. ABSTRACT

During the fourth quarter of the LRSCA program, detail drawings of the orientation mechanism were completed, incorporation of reference solar cell and solar cell modules of 8 and 12-mil cells in the solar panel design was begun, detail drawings of the drum mechanism and solar array neared completion, and all electronic circuit detail design was completed. Breadboards of the solar panel switch and charge current controller were built and tested over anticipated orbital temperature extremes. The boom actuator breadboard and engineering models were completed and tested by Spar Aerospace Corporation.

A power management summary was prepared and the preliminary "Performance, Design, and Product Confirmation Requirements for HS-207 Large Retractable Solar Cell Array Experiment" and the "Interface Requirements for HS-207 Large Retractable Solar Cell Array Experiment" were revised to reflect the present LRSCA design.

Uncertainties regarding the array dynamics and control/structural interactions were resolved. The system dynamic characteristics and Hughes analytic treatment of this field were reviewed for the Working Group on Flexible Vehicle Dynamic Interactions of the Joint USA/United Kingdom Technical Coordination Program (M-4) as the LRSCA semiannual presentation.

Coordination with LMSC, the integration contractor, was initiated 17 June 1969.

DD FORM 1 NOV 65 1473

UNCLASSIFIED
Security Classification